Bull. Natl. Mus. Nat. Sci., Ser. C, 50, pp. 7–26, December 20, 2024
DOI: 10.50826/bnmnsgeopaleo.50.0_7

Detrital zircon U–Pb ages of accretionary complexes in Amami-Oshima Island, central Ryukyu Arc, Japan

Yukiyasu Tsutsumi* and Kenichiro Tani

Department of Geology and Paleontology, National Museum of Nature and Science
4–1–1 Amakubo, Tsukuba, Ibaraki 305–0005, Japan
*Author for correspondence: ytsutsu@kahaku.go.jp

Abstract Although the zonal structure of basement accretionary complexes (ACs) in the Southwest Japan Arc has been thought to extend to the Ryukyu Arc, it is difficult to trace the continuity. We investigated detrital zircon U–Pb ages of sandstones from ACs in Amami-Oshima Island to establish their accretionary age and the continuity of the zonal structure in the central Ryukyu Arc. Basement ACs on Amami-Oshima Island were subdivided into the Yuwan, Naon and Amami Complexes. The Amami Complex shows detrital zircon age spectra similar to those of the older part in the northern Shimanto Belt. In contrast, the Naon Complex shows a spectrum like that of the Chichibu Belt. However, more than one zircon grain of about 110–100 Ma found in the Amami and Naon Complexes present that these complexes corresponding to the northern Shimanto Belt. The Naon Complex would not correspond to the Chichibu Belt as previously thought, but to the northern Shimanto Belt, and the Butsuzo Tectonic Line would be between the Yuwan and Naon Complexes.

Key words: detrital zircon, Butsuzo Tectonic Line, Chichibu Belt, Shimanto Belt, Amami-Oshima Island

Introduction

The basement of the Southwest (SW) Japan Arc shows a zonal structure of middle Carboniferous to Middle Miocene accretionary complexes (ACs) and metamorphosed ACs (meta-ACs) because of continuous accretion, subdivided into Inner and Outer Zones across the Median Tectonic Line (MTL). The Outer Zone is subdivided into the Jurassic Chichibu Belt, Cretaceous northern Shimanto Belt and Paleogene to Neogene southern Shimanto Belt from north to south, the boundaries being the Butsuzo Tectonic Line (BTL) and Aki Tectonic Line (ATL) (e.g., Isozaki *et al.*, 2010), except for the Cretaceous meta-AC of the Sanbagawa belt which crops out as a window along the southern side of the MTL (e.g., Knittel *et al.*, 2024) and the Kurosegawa Belt, which is thought to be the klippe of Inner Zone components and lies over the Chichibu Belt (e.g., Isozaki and Itaya, 1991) (Fig. 1).

The zonal structure of SW Japan has been thought to extend to the Ryukyu Arc (e.g., Konishi, 1963, 1965; Isozaki and Nishimura, 1989; Takami *et al.*, 1999). Only the southern Shimanto Belt outcrops in the northern Ryukyu Arc (e.g., Kuwazuru and Nagatsu, 2007; Saito *et al.*, 2007), while the Chichibu Belt and the northern and southern Shimanto Belts outcrop in the central Ryukyu Arc (Nakae *et al.*, 2010; Saito *et al.*, 2009; Takeuchi, 1994). In contrast, the Jurassic AC and Triassic meta-AC which outcrop in the southern Ryukyu Arc would originate from the Inner Zone of SW Japan (Isozaki and Nishimura, 1989). However, the ATL and BTL in the central Ryukyu Arc would be segmented into parts, and it is difficult to trace the continuity. Even in Amami-Oshima Island, in the northern part of the central Ryukyu Islands, the location of the BTL has varied in the literature (Fig. 2). Therefore, fixing the BTL in Amami-Oshima Island is the threshold to verifying a southern extension of the zonation.

To clarify the difference and/or affinity of the ACs between the central Ryukyu Arc and the SW Japan Arc, we investigated detrital zircon U–Pb ages of sandstones from ACs in Amami-Oshima Island. The detrital zircon ages taken from a sandstone sample could be used to infer its provenances (e.g., Hara *et al.*, 2017; Nakama *et al.*, 2010) and older limit of deposition ages (e.g., Dickinson and Gehrels, 2009). Because sandstone is a late sediment in an AC (Isozaki *et al.*, 1990), the older

© 2024 National Museum of Nature and Science

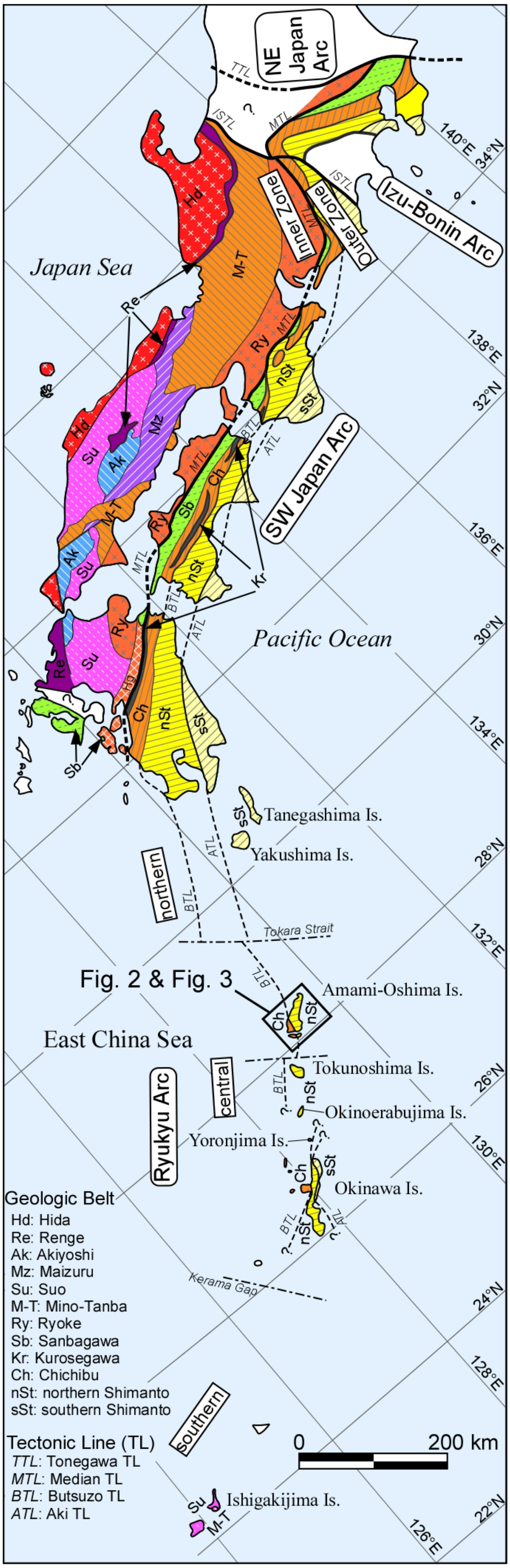

Fig. 1. Tectonic division map of SW Japan Arc and Ryukyu Arc.

limit of the deposition age of a sandstone sample indicates the older limit of the accretion age of the AC. Furthermore, the age data of this study will contribute to the validating of tectonic setting and transition of provenance of clastics around the central Ryukyu Arc.

Geological setting

The basement of Amami-Oshima Island consists of ACs which have been subdivided into geological units, but the names of those units and their boundaries vary slightly in the literature (e.g., Fujita, 1989; Kashima and Takahashi, 1977; Konishi, 1963; Osozawa *et al.*, 1983; Sakai *et al.*, 1977). In this study the names and boundaries of the geologic units follow Takeuchi (1994), being divided into the Yuwan, Naon and Amami Complexes (Fig. 3).

The Yuwan Complex consists mainly of basalt (greenstone), limestone, chert and mixed rock containing rocks listed above in a mudstone matrix. Sandstone is unevenly distributed and could not be collected in this study. Carboniferous–Permian fusulinidae were found from limestone in basaltic tuff breccia (Osozawa *et al.*, 1983) and Triassic conodonts were found from massive limestone (Igo, 1972). Although Permian-Triassic radiolarian assemblages are common in cherts, Late Jurassic radiolarian assemblages were reported from siliceous/tuffaceous shales and several cherts (Osozawa, 1986). Considering the above, for the Yuwan Complex it is supposed that the Late Jurassic AC contains Carboniferous-Permian basaltic rocks, Triassic massive limestones, Permian to Early Jurassic cherts, and Late Jurassic cherts and siliceous shales. These age signatures indicate that the Yuwan Complex would correspond to the Chichibu Belt.

The Naon Complex shows a blocks-in-matrix structure; blocks consist of basalt (greenstone), limestone, chert, siliceous shale and mudstone, and a matrix consisting of mudstone and sandstone. Huge blocks called “slabs” are often observed, with thicknesses of over 50 m (Takeuchi, 1993). Permian fusulinidae and coral and Triassic conodonts were found from limestones (Osozawa, 1986). Although Permian–Jurassic radiolarian assemblages were commonly observed in cherts (e.g., Osozawa, 1986;

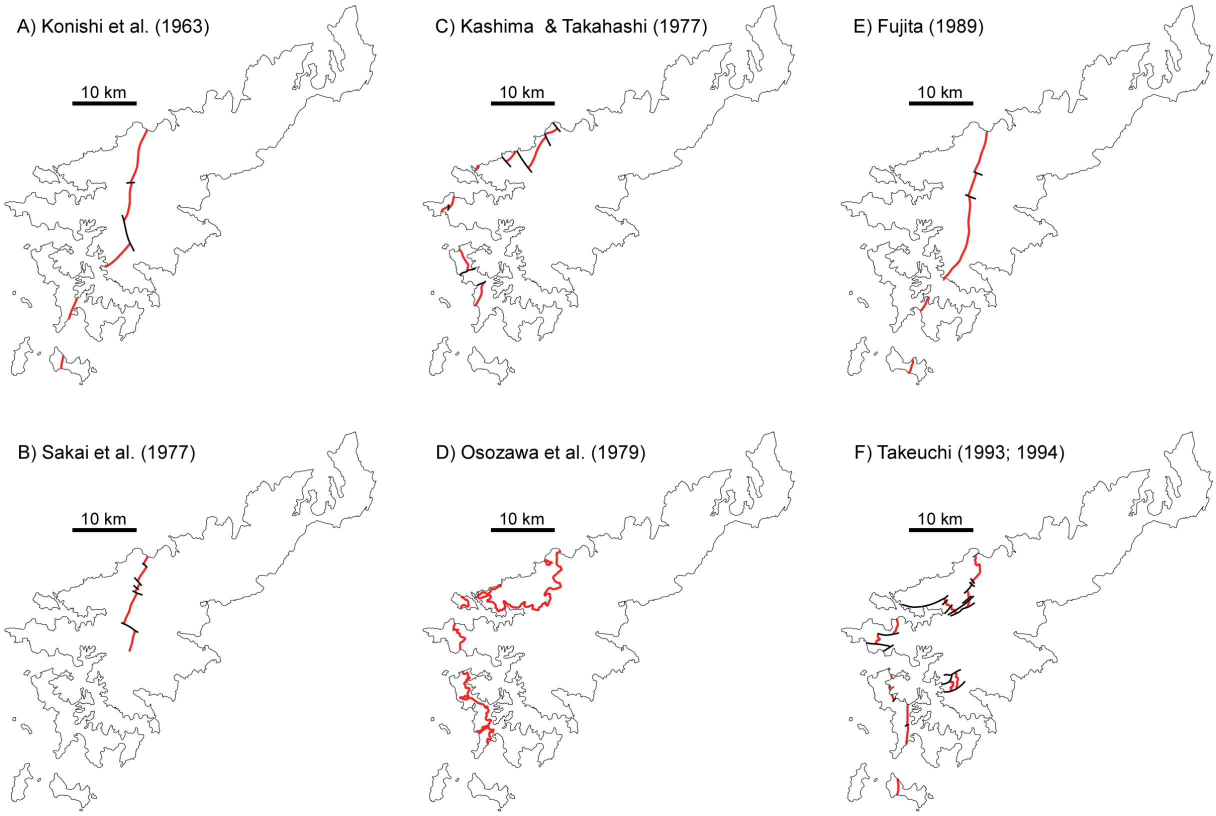

Fig. 2. Transition of the BTL locations in various studies.

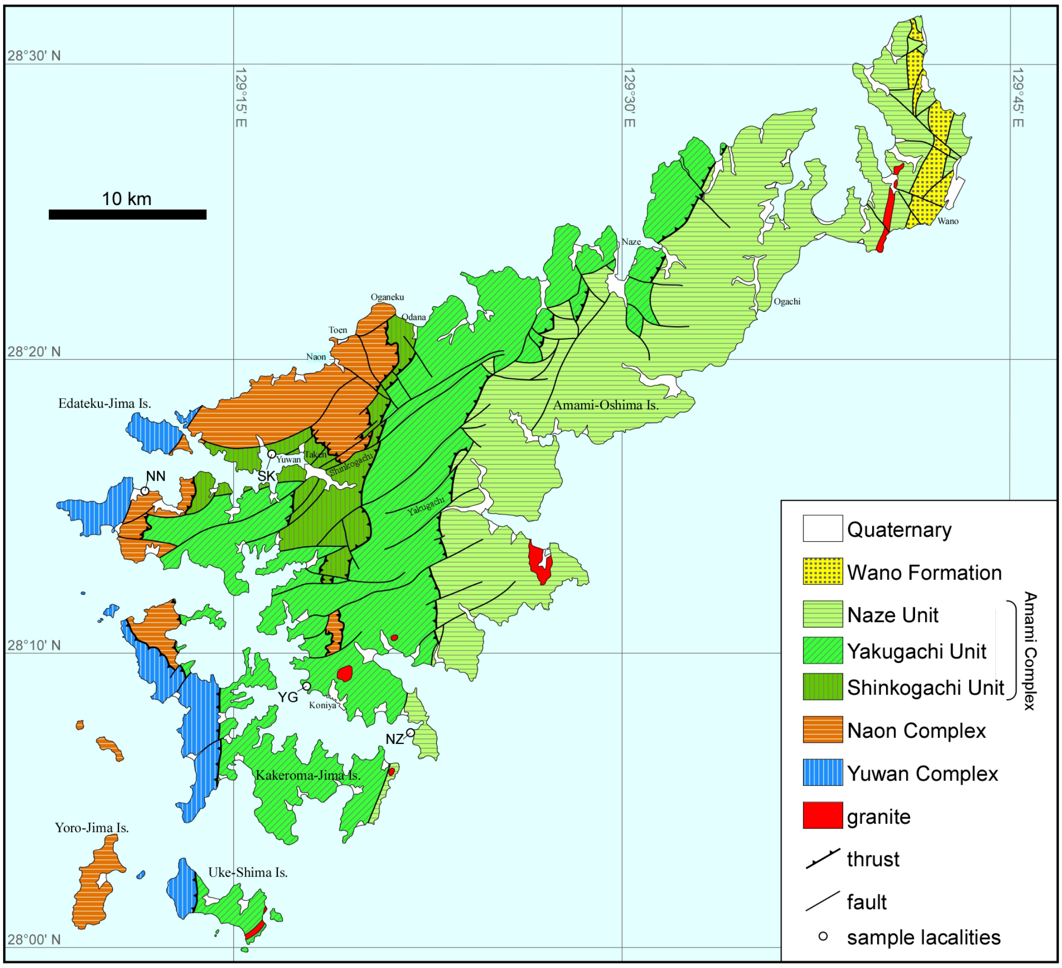

Fig. 3. Geological map of Amami-Oshima and surrounding islands with sample localities, modified after Takeuchi (1994).

Fujita, 1989), Early Cretaceous radiolarian assemblages were observed in several cherts and siliceous shales (Fujita, 1989). The ages of each rock type in the Yuwan and Naon Complexes are similar, except for the youngest age signature in the Naon Complex. Considering the above, the Naon complex is supposed to be an Early Cretaceous AC, and would correspond to the Sanbosan Unit, the southernmost part of the Chichibu Belt (e.g., Takeuchi, 1992; 1993). However, for the Naon Complex there is no report of microfossil ages from matrix mudstone and sandstone. It is possible that the accretion age of the Naon Complex is younger than the youngest microfossil ages.

The Amami Complex is subdivided into the Shinkogachi, Yakugachi and Naze Units from north to south; i.e., from tectonically upper to lower. The Shinkogachi Unit consists mainly of sandstone, mudstone and siliceous mudstone, and sometimes features slabs consisting of chert and greenstone which originated in the Chichibu Belt (Takeuchi, 1993). Although some previous studies thought this Unit to correspond to the Chichibu Belt, based on age signatures from the slabs (Fujita, 1986; Konishi, 1963; Sakai *et al.*, 1977; Fig. 2A, B, E), the youngest radiolarian fossil assemblage indicates Early to Late Albian (Fujita, 1986), which would be older limit of the accretion age of the Unit (Takeuchi, 1993). The Yakugachi and Naze Units consist of sandstone, mudstone, acidic tuff and greenstone, with no slabs originating from the Chichibu Belt (Takeuchi, 1993). The youngest radiolarian fossil assemblage of siliceous sandstone from the Yakugachi Unit indicates Albian to Turonian (Osozawa *et al.*, 1983; Takeuchi, 1993), which would be the accretion age. The only index fossil from the Naze Unit is late Cenomanian to early Turonian ammonite from sandstone–mudstone alternation (Ishikawa and Yamaguchi, 1965), which would be the accretion age. In addition to the fossil age evidences younger than Albian, Takeuchi (1992) detrital indicate that provenances of clastics are different between the Koniya and Naze Complexes (Amami Complex in this study) and Yuwan Complex (Yuwan and Naon Complexes in this study) using garnet compositions and sandstone components. Therefore, all Units of the Amami Complex would correspond to the Shimanto Belt.

There are five granitic provinces in SW Japan (e.g., Nakajima, 2018): the Hida (Permian to Jurassic), San-in (latest Cretaceous to Paleogene), San-yo (Cretaceous), Ryoke (Cretaceous) and Gaitai (Middle Miocene) Provinces from north to south; i.e., from continentalward to trenchward. The Shimanto Belt in the SW Japan Arc is involved in the Gaitai Province, where the ages of the granitoids are Middle Miocene (15.6–13.5 Ma; Shinjoe *et al.*, 2019). In contrast, the ages of the granitoids in the Amami Complex are Paleocene (65.9–61.7 Ma; Ogasawara and Fukuyama, 2017), which ages correspond to the San-in Province in the SW Japan Arc, situated about 200 km continentalward from the Gaitai Province.

Analytical methods

All sample preparation and analyses were conducted at National Museum of Nature and Science, Tsukuba, Japan. The rock samples were scrubbed and washed in an ultrasonic bath for ten minutes to avoid surface zircon contaminants as much as possible. Fragmentation of the rock samples was conducted by a high voltage pulse power selective fragmentation equipment, SELFRAG Lab (Selfrag AG). The zircon grains were handpicked from heavy fractions that were separated from heavy-liquid techniques. Zircon grains from the samples, the zircon standards FC1 (1099 Ma; Paces and Miller, 1993) and OD-3 (33 Ma; Iwano *et al.*, 2013), and the glass standard NIST SRM610 were mounted in an epoxy resin and polished till the surface was level with the center of the embedded grains. After mounting and polishing, backscattered electron and cathodoluminescence (CL) images of zircon grains were taken. A scanning electron microscope-cathodoluminescence equipment, JSM-6610 (JEOL) and a CL detector (SANYU electron), was used for CL images. The images were used to select suitable sites for analysis. U–Pb dating of these samples was carried out using a Laser Ablation Inductively Coupled Plasma Mass Spectrometer (LA-ICP-MS) that was composed of NWR213 (Elemental Scientific Lasers) and Agilent 7700x (Agilent Technologies). The experimental conditions and the analytical procedures for the measurements were after Tsutsumi *et al.* (2012), and additional devices of buffered type stabilizer (Tunheng and Hirata, 2004) and TwoVol2 sample cell were applied. The spot size of the laser was 25 µm. A correction for common Pb was made on the basis of the measured ^{208}Pb/^{206}Pb and Th/U ratios (^{208}Pb correction; e.g. Williams, 1998) and the model for common Pb compositions proposed by Stacey and Kramers (1975). ^{238}U/^{206}Pb* and ^{207}Pb*/^{206}Pb* ratios which corrected by ^{208}Pb correction are used for the concordia plot. Pb* indicates radiometric Pb. The criteria of concordant is for 2σ overlap of the concordia curve on a concordia diagram when ^{238}U–^{206}Pb* age is less than 1000 Ma, and discordancy (Song *et al.*, 1996) of less than 15% when ^{238}U–^{206}Pb* age more than and equal to 1000 Ma. ^{238}U–^{206}Pb* ages are used for less than 1000 Ma data and ^{207}Pb*/^{206}Pb* ages are used for the other data. The data of secondary standard OD-3 zircon obtained during analysis yielded weighted mean ages of 33.1 ± 1.4 Ma (n = 9; MSWD = 1.87; when NAZ was analyzed), 33.6 ± 1.6 Ma (n = 9; MSWD = 2.04; when YKG was analyzed), 31.0 ± 1.0 Ma (n = 10; MSWD = 0.96; when SKG was analyzed) and 31.4 ± 0.8 Ma (n = 9; MSWD = 0.47; when NAN was analyzed). MSWD is an acronym of mean square weighted deviation, calculated from the square root of the χ^2 value.

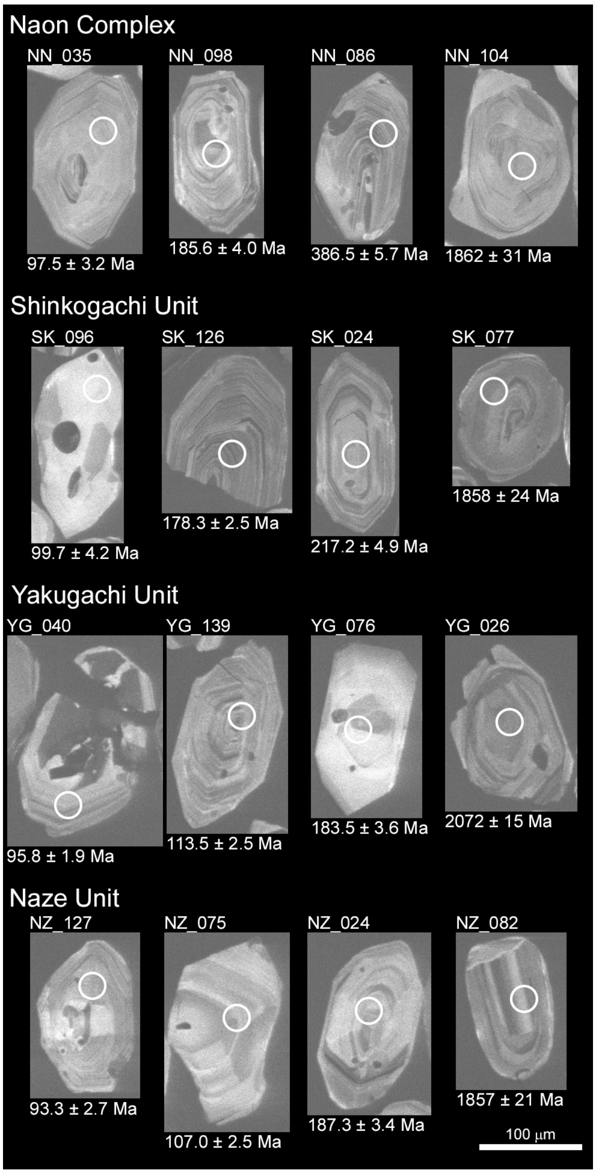

Fig. 4. Cathodoluminescence (CL) images of analyzing sections of typical zircon grains from the samples. Circles indicate analyzed spots by LA-ICP-MS. Spot diameter is 25 µm approx.

Sample descriptions and results of zircon age analysis

Table A1 lists zircon data in terms of the fraction of common ^{206}Pb, U and Th concentrations, Th/U, ^{238}U/^{206}Pb* and ^{207}Pb*/^{206}Pb* ratios, and radiometric ^{238}U–^{206}Pb* ages of the samples. All errors are of 1σ level. All zircons in the samples show rhythmic oscillatory and/or sector zoning on CL images (Fig. 4), which is commonly observed in igneous zircons (e.g., Corfu *et al.*, 2003). Concordia diagrams for each sample are shown in Fig. 5. The youngest single grain age (YSG) and the weighted mean of the youngest cluster of more than two grain ages that overlap in age within a 1σ error (YC1σ) (Dickinson and Gehrels, 2009) are commonly used to show the older limit of deposition age. All rock samples are stored at the National Museum of Nature and Science. The registration number of each sample is the catalogue number of the rock specimen in the collection database of the National Museum of Nature and Science (http://db.kahaku.go.jp/webmuseum_en/). The sample localities, registration numbers, YSG and YC1σ are summarized in Table 1. The geologic time scale in this study follows Gradstein and Ogg (2020).

NZ: Naze Unit, Amami Complex

The sample is a coarse-grained sandstone collected from the southernmost part of Sokaru, Setouchi Town, Amami-Oshima Island (lat. N28°07′33.9″, long. E129°21′37.2″). The registration number is 137279. A total of 146 spots/grains were analyzed and 135 data were found to be con-

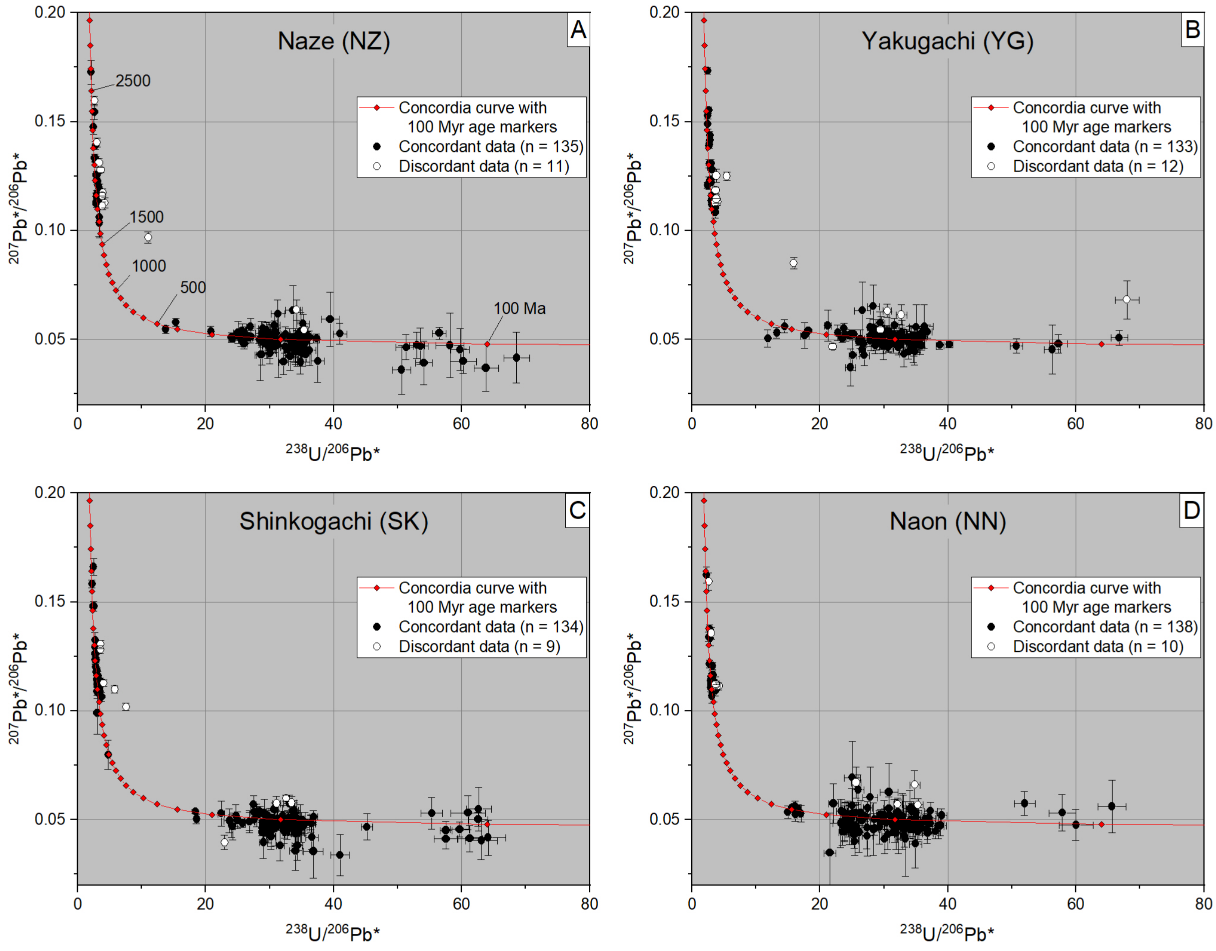

Fig. 5. Tera-Wasserberg U–Pb concordia diagrams of zircons from the samples.

Table 1. Summary of localities, registration numbers and indicators of older limit of deposition age of each sample.

Sample	Sample attribution	Locality	Reg. No.	n of data		YSG	YC1σ		
				All	Conc.	Age (Ma)	Age (Ma)	n	MSWD
NZ	Naze Complex	N 28°07′33.9″, E129°21′37.2″	137279	146	135	93.3 ± 2.7	102.7 ± 2.3	2	1.60
YK	Yakugachi Complex	N 28°09′09.0″, E129°17′45.8″	137280	145	133	95.8 ± 1.9	112.7 ± 1.8	2	0.26
SK	Shinkogachi Complex	N 28°16′57.8″, E129°16′24.1″	137281	143	134	99.7 ± 4.2	102.4 ± 1.4	6	0.22
NN	Naon Complex	N 28°15′46.0″, E129°11′27.1″	137283	148	138	97.5 ± 3.2	108.8 ± 3.0	2	0.41

Errors are 1σ
Conc.: concordant

cordant (Fig. 5A). The concordant age data form clusters at about 93–126 Ma (11 data), 155 Ma (1 datum), 161–262 Ma (4 data), 302 Ma (1 datum), 406 Ma (1 datum), 452 Ma (1 datum) and 33 data of Precambrian grains (Fig. 6A). There are prominent peaks at about 180 Ma and 220 Ma. The YSG and YC1σ of this sample are 93.3 ± 2.7 Ma (Cenomanian to Turonian) and 102.7 ± 2.3 Ma (Albian), respectively.

YK: Yakugachi Unit, Amami Complex

The sample is a coarse-grained sandstone collected from the southern part of Tean, Setouchi Town, Amami-Oshima Island (lat. N28°09′09.0″, long. E129°17′45.8″). The registration number is 137280. A total of 145 spots/grains were analyzed and 133 data were found to be concordant (Fig. 5B). The concordant age data form clusters at about 95–126 Ma (4 data), 158–277 Ma (94 data), 297 Ma (1 datum), 345 Ma (1 datum), 355 Ma (1 datum), 430 Ma (1 datum), 468 Ma (1 datum), 521 Ma (1 datum) and 29 data of Precambrian grains (Fig. 6B). The YSG and YC1σ of this sample are 95.8 ± 1.9 Ma (Cenomanian) and 112.7 ± 1.8 Ma (Aptian to Albian), respectively.

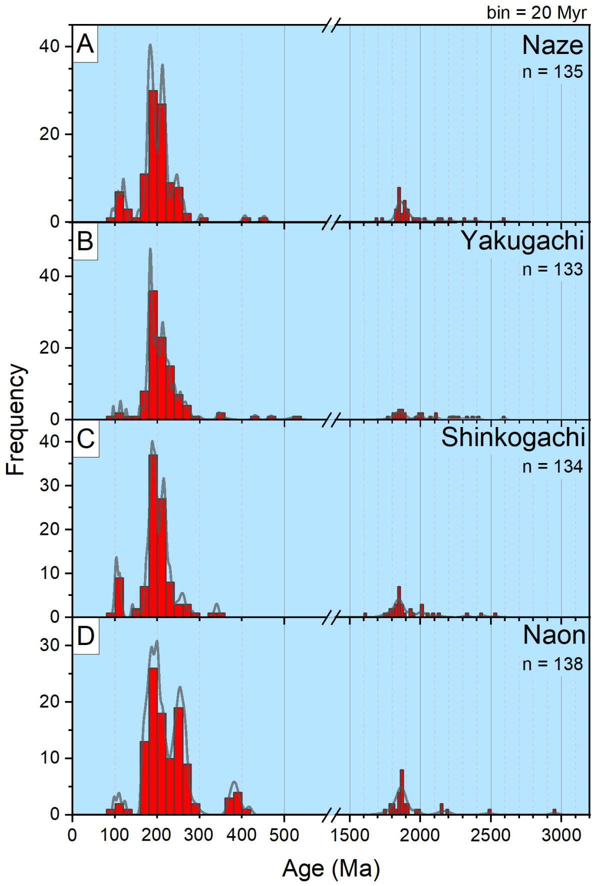

Fig. 6. Probability distribution diagrams and histograms of concordant ages from the samples.

SK: Shinkogachi Unit, Amami Complex

The sample is a medium-grained sandstone collected from the southeastern part of Ashiken, Setouchi Town, Amami-Oshima Island (lat. N28°16′57.8″, long. E129°16′24.1″). The registration number is 137281. A total of 143 spots/grains were analyzed and 134 data were found to be concordant (Fig. 5C). The concordant age data form clusters at about 100–116 Ma (10 data), 141 Ma (1 datum), 155 Ma (1 datum), 173–281 Ma (86 data), ~340 Ma (2 data) and 34 data of Precambrian grains (Fig. 6C). The YSG and YC1σ of this sample are 99.7 ± 4.2 Ma (Albian to Cenomanian) and 102.4 ± 1.4 Ma (Albian), respectively.

NN: Naon Complex

The sample is a coarse-grained sandstone collected from the eastern part of Yadon, Setouchi Town, Amami-Oshima Island (lat. N28°15′46.0″, long. E129°11′27.1″). The registration number is 137283. A total of 148 spots/grains were analyzed and 138 data were found to be concordant (Fig. 5D). The concordant age data form clusters at about 98–123 Ma (4 data), 163–292 Ma (97 data), 367–416 Ma (8 data) and 29 data of Precambrian grains (Fig. 6D). The YSG and YC1σ of this sample are 97.5 ± 3.2 Ma (Albian to Cenomanian) and 108.8 ± 3.0 Ma (Albian), respectively.

Discussion

Accretion age for each accretionary unit

Although YSG should indicate the older limit of the depositional age in principle, YC1σ is commonly better than YSG in doing so because estimates based on ages from multiple grains are more consistent (Dickinson and Gehrels, 2009). The YC1σ of this study is detached from YSG for each sample because of the low amount of age data in the youngest age cluster, except for the SK sample. It would indicate the presence of a 'real youngest cluster' around YSG which could not be found because of shortage of data, despite a sufficient quantity to meet the requisite condition (Vermeesch, 2004). Therefore, the accretion age of the accretionary units in this study should be comprehensively considered using YSG, YC1σ and index/radiolarian fossils. All errors in this study are 1σ.

Naze Unit: The YSG and YC1σ of this NZ sample are 93.3 ± 2.7 Ma (Cenomanian to Turonian) and 102.7 ± 2.3 Ma (Albian), respectively. The only index fossil age from the latest sediments of the unit is late Cenomanian to early Turonian (Ishikawa and Yamaguchi, 1965). The younger zircon age data of the NZ sample are of insufficient quantity to form a youngest age cluster, and it is not effective to restrict the older limit of deposition age. Therefore, 'late Cenomanian to early Turonian,' which is restricted using the index fossil and consistent to the YSG, would be acceptable for the accretion age.

Yakugachi Unit: The YSG and YC1σ of the YK sample indicate 95.8 ± 1.9 Ma (Cenomanian) and 112.7 ± 1.8 Ma (Aptian to Albian), respectively, while the youngest radiolarian fossil assemblage from a sandstone indicates Albian to Turonian (Osozawa *et al.*, 1983; Takeuchi, 1993). Because the YC1σ is clearly isolated from the YSG and is clearly older than the fossil age, it is not effective to restrict the older limit of the accretion age for the YK sample. Therefore, 'late Cenomanian to Turonian,' which is restricted using the radiolarian fossil assemblage, YSG, and estimated accretion age of the Naze Unit, would be acceptable for the accretion age.

Shinkogachi Unit: The youngest radiolarian fossil assemblage indicates Early to Late Albian (Fujita, 1986), while the YSG and YC1σ of zircon U–Pb ages from the SK sample indicate 99.7 ± 4.2 Ma (Albian to Cenomanian) and 102.4 ± 1.4 Ma (Albian), respectively. It is possible that the accretion age is Cenomanian and after. Considering YSG data, 'on and after latest Albian' would nonetheless be better, strictly speaking.

Naon Complex: The youngest fossil remarks are Early Cretaceous radiolarian assemblages (Fujita, 1989). Additionally, the YSG and YC1σ of zircon U–Pb ages from the NN sample indicate 97.5 ± 3.2 Ma (Albian to Cenomanian) and 108.8 ± 3.0 Ma, respectively. These age data restrict the accretion age of the Naon Complex to at least on or after Early Albian. Although it is possible that the accretion age is Cenomanian and after, considering the YSG, 'on and after Albian' would strictly be better. Additionally, the age signatures demonstrate that the Naon Complex would correspond to the northern part of the Northern Shimanto Belt rather than the Sanbosan Unit, southernmost in the Chichibu Belt, where the youngest radiolarian assemblage indicates late Valanginian to early Hauterivian (about 133 Ma) (Matsuoka *et al.*, 1998). Therefore, the BTL would be between the Yuwan and Naon Complexes.

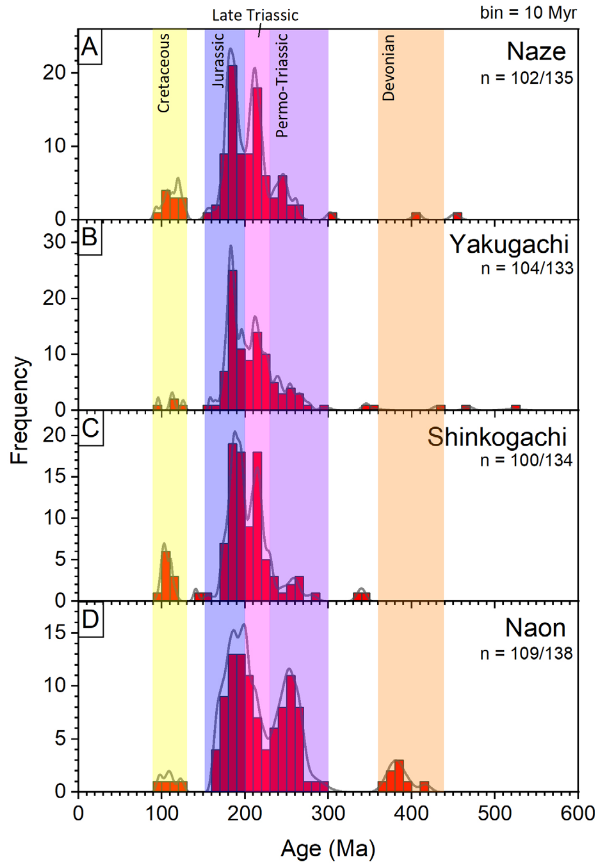

Fig. 7. Probability distribution diagrams and histograms of concordant ages from the samples in the Phanerozoic range.

Interpretation of the zircon age spectra

The zircon age spectra of the NZ, YK and SK samples have prominent peaks at the Late Triassic and Jurassic and small peaks at the Permo-Triassic and Cretaceous (Fig. 7A, B, C). These spectra are similar to those of the northern part of the Northern Shimanto Belt, the Tochidani, Hinotani and Osodani Units in Shikoku (Hara *et al.*, 2017). Comparatively, the age spectrum of the NN sample has prominent peaks at the Permo-Triassic and Jurassic, and a small peak at the Devonian (Fig. 7D). Although this spectrum is similar to those of the Chichibu Belt (Tokiwa *et al.*, 2019), more than one Cretaceous zircon grain and the shoulder of the peak at the Late Triassic would reflect incorporation of northern Shimanto components. The Naon Complex shows a block-in-matrix texture and the NN sample is a sandstone from the matrix. The origin of clastics in the matrix sandstones of the Naon Complex would be tectonic eroded and weathered Chichibu Belt and Cretaceous trench-fill sediments.

The youngest age clusters of zircons in the samples from Amami-Oshima Island are far lower in quantity than those from Shikoku. This fact indicates less igneous activity around the central Ryukyu Arc, compared to the SW Japan Arc, during the middle Cretaceous. Additionally, the zircon age spectra of the samples have no age signature of the South China Craton (SCC), which was prominent around 600 Ma to 1000 Ma (e.g., Xu *et al.*, 2007, Zhou *et al.*, 2002) in spite of neighboring the SCC. This information will be a clue in solving the tectonics around the East China Sea.

Conclusions

The zonal structure of basement ACs in the SW Japan Arc continue to the Ryukyu Arc (Fig. 1), but the location of the BTL is still not certain even on Amami-Oshima Island, in the northern part of the central Ryukyu Islands (Fig. 2). The basement of Amami-Oshima Island consists of Acs which were divided to the Yuwan, Naon and Amami Complexes. The Amami Complex was subdivided into the Shinkogachi, Yakugachi and Naze Units from north to south; i.e., from tectonically upper to lower (Fig. 3). Detrital zircon U–Pb dating is applied to sandstones from these ACs to clarify the continuity between the central Ryukyu and SW Japan Arcs.

Most detrital zircon grains from the samples are igneous in origin (Fig. 4) and indicate concordant age (Fig. 5). The indexes of the older limit of accretion age (YSG and/or YC1σ) for the samples indicate 113–93 Ma (Albian to Turonian) (Table 1), being much younger than the age of the Sanbosan Unit, southernmost in the Chichibu Belt, which is late Valanginian to early Hauterivian (about 133 Ma) in age. The accretionary ages, estimated comprehensively using detrital zircon age data and index/radiolarian fossils data of the Naon Complex and Shinkogachi, Yakugachi and Naze Units, are estimated as: Albian and after, late Albian and after, late Cenomanian to Turonian and late Cenomanian to early Turonian, respectively.

The age spectra of detrital zircons for the samples show roughly bimodal results; Phanerozoic and older than Mesoproterozoic, without Neoproterozoic (Fig. 6). The Phanerozoic range of the spectra of the Units in the Amami Complex (Fig. 7A, B, C) is similar to the older (northern) part of the northern Shimanto Belt while that of the Naon Complex (Fig. 7D) is similar to the Chichibu Belt. Clastics in the sandstone of the Naon Complex would originate from tectonically eroded and weathered Chichibu Belt and Cretaceous trench-fill sediments, and the accretion age corresponds to the northern Shimanto Belt. Therefore, the BTL would be between the Yuwan and Naon Complexes.

Acknowledgment

The authors thank Mrs. Y. Kusaba of the National Museum of Nature and Science for her help in SEM analysis. This work is conducted as a part of the project “Interpretation of distribution (condensation and diffusion) of rare metals in igneous rocks” of National Museum of Nature and Science.

References

Corfu, F., Hanchar, J. M., Hoskin, P. W. O. and Kinny, P. (2003) An atlas of zircon textures. In: Hanchar, J. M. and Hoskin, P. W. O. (Ed.), *Zircon: Reviews in Mineralogy and Geochemistry 53*, Mineralogical Society of America, Washington D.C., USA: 469–500.

Dickinson, W. R. and Gehrels, G. E. (2009) Use of U–Pb ages of detrital zircons to infer maximum depositional ages of strata: A test against a Colorado Plateau Mesozoic database. *Earth and Planetary Science Letters*, **288**: 115–125.

Fujita, H. (1989) Stratigraphy and geologic structure of the pre-Neogene strata in central Ryukyu Islands. *Journal of Science of Hiroshima University Ser. C*, **9**: 237–284.

Gradstein F. M. and Ogg, J. G. (2020) Chapter 2: The chronostratigraphic scale. In: Gradstein, F. M., Ogg, J. G., Schmitz, M. D. and Ogg, G. M., (Ed.), *Geologic Time Scale 2020*, *Vol. 1*, Elsevier, 159–192.

Hara, H., Nakamura, Y., Hara, K., Kurihara, T. Mori, H., Iwano, H., Danhara, T. Sakata, S. and Hirata, T. (2017) Detrital zircon multi-chronology, provenance, and low-grade metamorphism of the Cretaceous Shimanto accretionary complex, eastern Shikoku, Southwest Japan: Tectonic evolution in response to igneous activity within a subduction zone. *Island Arc*, **26**: e12218.

Igo, H. (1972) Conodonts, as a new Index Fossil in Japan. *Journal of Geography (Chigaku Zasshi)*, **81**: 142–151 (in Japanese with English abstract).

Ishikawa, H. and Yamaguchi, S. (1965) On the discovery of Ammonite from Honto Isl., of Amami-Oshima, Ryukyu and its geological meaning. *Journal of the Geological Society of Japan*, **71**: 78–79 (in Japanese).

Isozaki, Y., Aoki, K., Nakama, T. and Yanai, S. (2010) New insight into a subduction-related orogen: A reappraisal of the geotectonic framework and evolution of the Japanese Islands. *Gondwana Research*, **18**: 82–105.

Isozaki, Y. and Itaya, T. (1991) Pre-Jurassic klippe in northern Chichibu belt in west-central Shikoku, Southwest Japan. *Journal of the Geological Society of Japan*, **97**: 431–450 (in Japanese with English abstract).

Isozaki, Y. and Nishimura, Y. (1989) Fusaki Formation, Jurassic subduction–accretion complex on Ishigaki Island, southern Ryukyus and its geologic implication to Late Mesozoic convergent margin of East Asia. *Memoir of the Geological Society of Japan*, **33**: 259–275 (in Japanese with English abstract).

Iwano, H., Orihashi, Y., Hirata, T., Ogasawara, M., Danhara, T., Horie, K., Hasebe, N., Sueoka, S., Tamura, A., Hayasaka, Y., Katsube, A., Ito, H., Tani, K., Kimura, J., Chang, Q., Kouchi, Y., Haruta, Y. and Yamamoto, K. (2013) An inter-laboratory evaluation of OD-3 zircon for use as a secondary U–Pb dating standard. *Island Arc*, **22**: 382–394.

Kashima, N. (1983) Studies on the Butsuzo tectonic line of Ryukyu Arc. *Memoirs of Geological Society of Japan*, **22**: 57–65 (in Japanese with English abstract).

Kashima, N. and Takahashi, J. (1977) Stratigraphical sequence of Kakeroma-Island, Amami-archipelago with special concern to its syntectogenic sedimentation. In: Kizaki K. (Ed.), *Geological Studies of the Ryukyu Islands (Report of Grani-in-Aid for Scientific Research No. 234050)*, **2**: 25–33 (in Japanese with English abstract).

Knittel, U., Tokiwa, T, Tsutsumi, Y., Endo, S. and Wallis, S. R. (2024) Geochronology of the Sanbagawa Belt: Younger and faster than before. *Elements*, **20**, 89–95.

Konishi, K. (1963) Pre-Miocene basement complex of Okinawa, and the tectonic belts of the Ryukyu Islands. *Science Report of Kanazawa University*, **8**: 569–602.

Konishi, K. (1965) Geotectonic framework of the Ryukyu Islands. *Journal of the Geological Society of Japan*, **71**: 437–457 (in Japanese with English abstract).

Kuwazuru, J. and Nagatsu, M. (2007) Paleogene radiolarians from the Kumage Group in northern Tanegashima Island, Kagoshima Prefecture, Japan. *Bulletin of the Kagoshima Prefectural Museum*, **26**: 1–11 (in Japanese).

Matsuoka, A., Yamakita, S., Sakakibara, M. and Kisada, K. (1998) Unit division for the Chichibu Composite Belt from a view point of accretionary tectonics and geology of western Shikoku, Japan. *Journal of the Geological Society of Japan*, **104**: 634–653 (in Japanese with English abstract).

Nakae, S., Kaneko, N., Miyazaki, K., Ohno, T. and Komazawa, M. (2010) *Geological Map of Japan 1:200000*, *Yoron Jima and Naha*. Tsukuba, Japan: Geological Survey of Japan (in Japanese with English abstract).

Nakama, T., Hirata, T., Otoh, S., Aoki, K., Yanai, S., & Maruyama, S. (2010) Paleogeography of the Japanese Islands: Age spectra of detrital zircon and provenance history of the orogen. *Journal of Geography (Chigaku Zasshi)*, **119**: 1161–1172 (in Japanese with English abstract).

Ogasawara, M. and Fukuyama, M. (2017) Zircon U–Pb ages and Sr–Nd isotopes of granitoids in the Ryukyu Islands, Japan. *Abstracts of 124th Annual Meeting of the Geological Society of Japan*, **124**: R5-O-22 (in Japanese).

Osozawa, S., Aita, Y., Nakamori, T., Hashimoto, S., Minoura, K., Horiguchi, T. and Nakagawa, H. (1979) Geology of Amami Oshima, Amami Gunto—A preliminary report. In: Kizaki, K. (Ed.), *Geological Studies of the Ryukyu Islands (Report of Grani-in-Aid for Scientific Research No. 234050)*, **4**: 95–106 (in Japanese with English abstract).

Osozawa, S., Aita, Y., Nakamori, T., Niibe, A., Kanisawa, S. and Nakagawa, H. (1983) Geology of Amami Oshima, central part of the Ryukyu Islands, with special reference to effect of gravity transportation on geologic construction. *Memoirs of Geological Society of Japan*, **22**: 39–56 (in Japanese with English abstract).

Osozawa, S. (1986) Origin of chert, limestone and basalt complex in Japan. *Journal of the Geological Society of Japan*, **92**: 709–722 (in Japanese with English abstract).

Paces, J. B. and Miller, J. D. (1993) Precise U–Pb age of Duluth Complex and related mafic intrusions, northern Minnesota: geochronological insights to physical, petrogenetic, paleomagnetic, and tectonomagmatic processes associated with the 1.1 Ga midcontinent rift system. *Journal of Geophysical Research*, **98**: 13997–14013.

Saito, M., Kawakami, S. and Ogasawara, M. (2007) Establishment of stratigraphic framework of the Shimanto accretionary complex in Yakushima Island, Japan, based on newly found Eocene radiolarian fossils. *Journal of the Geological Society of Japan*, **113**: 266–269 (in Japanese with English abstract).

Saito, M., Ozaki, M., Nakano, S., Kobayashi, T. and Komazawa, M. (2009) *Geological Map of Japan 1:200000*, *Tokunoshima*. Tsukuba, Japan: Geological Survey of Japan (in Japanese with English abstract).

Sakai, T., Ono, K., Momoki, Y., Otsuka, H. and Hayasaka, S. (1977) Geology of northern part of the Amami-Oshima. In: Kizaki, K. (Ed.), *Geological Studies of the Ryukyu Islands (Report of Grani-in-Aid for Scientific Research No. 234050)*, **2**: 11–23 (in Japanese with English abstract).

Shinjoe, H., Orihashi, Y. and Anma, R. (2021) U–Pb ages of Miocene near-trench granitic rocks of the Southwest Japan arc: Implications for magmatism related to hot subduction. *Geological Magazine*, **158**: 47–71.

Song, B., Nutman, A. P. Liu, D. and Wu, J. (1996) 3800 to 2500 Ma crustal evolution in the Anshan area of Liaoning Province, northeastern China. *Precambrian Research*, **78**, 79–94.

Stacey, J. S. and Kramers, J. D. (1975) Approximation of terrestrial lead isotope evolution by a two-stage model. *Earth and Planetary Science Letters*, **26**: 207–221.

Takami, M., Takemura, R., Nishimura, Y. and Kojima, T. (1999) Reconstruction of oceanic plate stratigraphies and unit division of Jurassic-Early Cretaceous accretionary complexes in the Okinawa Islands, central Ryukyu Island Arc. *Journal of the Geological Society of Japan*, **105**: 866–880 (in Japanese with English abstract).

Takeuchi, M. (1992) Origin of detrital garnet from the Mesozoic sandstones of Amami-Oshima, Nansei Islands. *Memoirs of Geological Society of Japan*, **38**: 237–248 (in Japanese with English abstract).

Takeuchi, M. (1993). *Geology of the Yuwan district. Quadrangle Series 1:50000*. Tsukuba, Japan: Geological Survey of Japan (in Japanese with English abstract).

Takeuchi, M. (1994) *Geological Map of Japan 1:200000*, *Amami-Oshima*. Tsukuba, Japan: Geological Survey of Japan (in Japanese with English legend).

Tokiwa, T., Shimura, Y., Takeuchi, M., Shimosato, S., Yamamoto, K. and Mori, H. (2019) Provenance of trench-fill deposits of the Jurassic Chichibu accretionary complex, Southwest Japan. *Journal of Asian Earth Sciences*, **184**: 103970.

Tsutsumi, Y., Horie, K., Sano, T., Miyawaki, R., Momma, K., Matsubara, S., Shigeoka, M. and Yokoyama, K. (2012) LA-ICP-MS and SHRIMP ages of zircons in chevkinite and monazite tuffs from the Boso Peninsula, Central Japan. *Bulletin of the National Museum of Nature and Science*, *Series C*, **38**: 15–32.

Tunheng, A and Hirata, T. (2004) Development of signal smoothing device for precise elemental analysis using laser ablation-ICP-mass spectrometry. *Journal of Analytical Atomic Spectrometry*, **7**: 932–934.

Vermeesch, P. (2004) How many grains are needed for a provenance study? *Earth and Planetary Science Letters* **224**: 441– 451

Williams, I. S. (1998) U–Th–Pb geochronology by ion microprobe. In: McKibben, M. A., Shanks, W. C. P. and Ridley, W. I. (Ed.), *Applications of Microanalytical Techniques to Understanding Mineralizing Processes. Reviews in Economic Geology 7*, Society of Economic Geologists, Littleton, CO. USA: 1–35.

Xu, X., O'Reilly, S. Y., Griffin, W. L., Wang, X, Pearson, N. J. and He, Z. (2007) The crust of Cathaysia: Age, assembly and reworking of two terranes. *Precambrian Research*, **158**: 51–78.

Zhou, M.-F., Yan, D.-P., Kennedy, A. K., Li, Y. and Ding, J. (2002) SHRIMP U–Pb zircon geochronological and geochemical evidence for Neoproterozoic arc-magmatism along the western margin of the Yangtze Block, South China. *Earth and Planetary Science Letters*, **196**: 51–67.

Appendix

Table A1. LA-ICP-MS U–Pb data and calculated ages of zircons in the samples.

Labels	$^{206}Pb_c$ (1) (%)	U (ppm)	Th (ppm)	Th/U	$^{238}U/^{206}Pb^{*(1)}$	$^{207}Pb^{*}/^{206}Pb^{*(1)}$	$^{238}U/^{206}Pb^{*}$ age(1) (Ma)	$^{207}Pb^{*}/^{206}Pb^{*}$ age(1) (Ma)	Disc (2) (%)	Remarks
NZ_001	0.59	359	515	1.47	54.09 ± 1.28	0.0393 ± 0.0100	118.1 ± 2.8			
NZ_002	0.12	326	153	0.48	3.35 ± 0.04	0.1311 ± 0.0020	1683.7 ± 19.8	2114 ± 26	20.35	discordant
NZ_003	0.00	52	24	0.48	25.09 ± 0.73	0.0532 ± 0.0051	251.9 ± 7.2			
NZ_004	0.15	496	117	0.24	3.04 ± 0.03	0.1135 ± 0.0014	1835.6 ± 17.8	1857 ± 22	1.15	
NZ_005	0.12	538	178	0.34	30.02 ± 0.45	0.0489 ± 0.0026	211.3 ± 3.1			
NZ_006	0.00	249	221	0.91	30.19 ± 0.51	0.0481 ± 0.0025	210.1 ± 3.5			
NZ_007	0.00	296	103	0.36	3.27 ± 0.04	0.1153 ± 0.0014	1718.7 ± 17.1	1886 ± 21	8.87	
NZ_008	0.95	236	160	0.69	34.36 ± 0.83	0.0444 ± 0.0067	185.0 ± 4.4			
NZ_009	0.34	519	199	0.39	35.39 ± 0.54	0.0523 ± 0.0030	179.6 ± 2.7			
NZ_010	0.00	195	148	0.78	26.04 ± 0.49	0.0481 ± 0.0024	243.0 ± 4.5			
NZ_011	1.38	203	199	1.01	63.81 ± 1.92	0.0369 ± 0.0108	100.2 ± 3.0			
NZ_012	0.86	77	124	1.65	3.38 ± 0.06	0.1062 ± 0.0089	1672.0 ± 25.8	1735 ± 148	3.63	
NZ_013	0.25	255	332	1.34	53.59 ± 1.17	0.0470 ± 0.0083	119.2 ± 2.6			
NZ_014	0.16	335	239	0.73	34.56 ± 0.63	0.0485 ± 0.0050	183.9 ± 3.3			
NZ_015	0.53	270	198	0.75	34.01 ± 0.69	0.0499 ± 0.0051	186.8 ± 3.7			
NZ_016	0.00	80	42	0.54	30.75 ± 0.85	0.0566 ± 0.0054	206.3 ± 5.6			
NZ_017	0.63	240	108	0.46	30.05 ± 0.56	0.0498 ± 0.0050	211.0 ± 3.9			
NZ_018	0.00	426	461	1.11	56.51 ± 1.06	0.0529 ± 0.0028	113.1 ± 2.1			
NZ_019	0.00	115	51	0.46	4.26 ± 0.06	0.1128 ± 0.0024	1358.1 ± 18.5	1845 ± 39	26.39	discordant
NZ_020	0.00	152	53	0.36	3.32 ± 0.05	0.1142 ± 0.0021	1696.4 ± 20.5	1868 ± 32	9.18	
NZ_021	0.00	305	277	0.93	13.77 ± 0.18	0.0547 ± 0.0018	452.1 ± 5.7			
NZ_022	0.50	78	49	0.65	39.46 ± 1.42	0.0593 ± 0.0125	161.3 ± 5.7			
NZ_023	0.38	96	70	0.75	2.50 ± 0.04	0.1476 ± 0.0034	2168.9 ± 27.4	2319 ± 39	6.47	
NZ_024	0.00	262	148	0.58	33.91 ± 0.62	0.0471 ± 0.0025	187.3 ± 3.4			
NZ_025	0.00	99	51	0.53	29.71 ± 0.75	0.0472 ± 0.0037	213.4 ± 5.3			
NZ_026	0.00	264	129	0.50	2.71 ± 0.03	0.1333 ± 0.0018	2023.8 ± 20.7	2143 ± 23	5.56	
NZ_027	0.72	769	443	0.59	2.89 ± 0.03	0.1319 ± 0.0020	1916.0 ± 18.8	2125 ± 26	9.83	
NZ_028	0.00	557	316	0.58	35.42 ± 0.55	0.0543 ± 0.0019	179.5 ± 2.8			discordant
NZ_029	0.00	263	127	0.50	3.09 ± 0.04	0.1134 ± 0.0014	1808.1 ± 20.8	1855 ± 23	2.53	
NZ_030	1.80	143	148	1.06	50.61 ± 1.43	0.0361 ± 0.0112	126.1 ± 3.5			
NZ_031	0.01	442	146	0.34	20.82 ± 0.32	0.0537 ± 0.0023	302.4 ± 4.5	357 ± 95	15.28	
NZ_032	0.00	183	97	0.54	32.48 ± 0.71	0.0524 ± 0.0034	195.5 ± 4.2	302 ± 143	35.27	
NZ_033	0.78	285	208	0.75	35.15 ± 0.69	0.0434 ± 0.0057	180.8 ± 3.5			
NZ_034	0.96	184	94	0.52	32.17 ± 0.72	0.0398 ± 0.0059	197.3 ± 4.3			
NZ_035	0.00	172	86	0.51	2.91 ± 0.04	0.1156 ± 0.0018	1904.9 ± 21.1	1890 ± 28	−0.79	
NZ_036	0.00	849	343	0.41	32.06 ± 0.44	0.0510 ± 0.0016	198.0 ± 2.7			
NZ_037	0.46	155	75	0.50	33.65 ± 0.68	0.0464 ± 0.0065	188.8 ± 3.8			
NZ_038	1.11	264	143	0.56	3.43 ± 0.06	0.1036 ± 0.0068	1648.9 ± 26.0	1690 ± 117	2.43	
NZ_039	0.00	822	542	0.68	3.22 ± 0.03	0.1150 ± 0.0011	1743.0 ± 15.1	1882 ± 17	7.38	
NZ_040	0.00	1052	57	0.06	29.17 ± 0.34	0.0513 ± 0.0016	217.3 ± 2.5			
NZ_041	0.00	149	96	0.66	11.03 ± 0.25	0.0968 ± 0.0027	559.5 ± 12.1	1565 ± 51	64.25	discordant
NZ_042	0.00	233	218	0.96	3.04 ± 0.04	0.1404 ± 0.0019	1831.2 ± 20.5	2234 ± 24	18.03	discordant
NZ_043	0.08	46	27	0.60	2.12 ± 0.05	0.1728 ± 0.0055	2493.3 ± 44.4	2586 ± 52	3.58	
NZ_044	1.21	143	43	0.31	30.82 ± 0.66	0.0538 ± 0.0048	205.9 ± 4.3			
NZ_045	0.00	323	300	0.95	29.75 ± 0.60	0.0500 ± 0.0024	213.1 ± 4.2			
NZ_046	0.54	438	67	0.16	3.96 ± 0.05	0.1174 ± 0.0016	1451.1 ± 16.1	1919 ± 24	24.38	discordant
NZ_047	0.00	168	150	0.91	28.94 ± 0.68	0.0551 ± 0.0033	219.0 ± 5.1			
NZ_048	0.00	97	70	0.75	29.91 ± 0.85	0.0481 ± 0.0045	212.0 ± 5.9			
NZ_049	0.08	266	171	0.66	34.89 ± 0.67	0.0523 ± 0.0056	182.1 ± 3.4			
NZ_050	0.00	86	71	0.84	51.34 ± 1.65	0.0465 ± 0.0059	124.3 ± 4.0			
NZ_051	0.00	417	321	0.79	29.88 ± 0.46	0.0519 ± 0.0022	212.2 ± 3.2			
NZ_052	0.00	600	368	0.63	28.40 ± 0.46	0.0499 ± 0.0018	223.1 ± 3.5			
NZ_053	0.27	260	94	0.37	33.22 ± 0.69	0.0465 ± 0.0046	191.2 ± 3.9			
NZ_054	0.00	139	72	0.53	3.39 ± 0.05	0.1169 ± 0.0022	1667.1 ± 23.2	1910 ± 34	12.72	
NZ_055	0.00	189	144	0.78	29.49 ± 0.62	0.0543 ± 0.0034	215.0 ± 4.4			
NZ_056	0.00	157	98	0.64	25.60 ± 0.51	0.0498 ± 0.0029	247.0 ± 4.9			
NZ_057	1.01	80	80	1.02	28.57 ± 0.87	0.0430 ± 0.0119	221.8 ± 6.6			
NZ_058	0.00	216	48	0.23	29.59 ± 0.60	0.0514 ± 0.0024	214.3 ± 4.3			
NZ_059	0.00	284	116	0.42	3.49 ± 0.06	0.1127 ± 0.0017	1625.9 ± 23.0	1845 ± 26	11.88	
NZ_060	0.00	898	332	0.38	24.91 ± 0.32	0.0515 ± 0.0020	253.7 ± 3.2			
NZ_061	0.00	307	101	0.34	3.07 ± 0.03	0.1226 ± 0.0014	1815.4 ± 17.8	1996 ± 20	9.05	
NZ_062	0.00	223	82	0.38	26.77 ± 0.56	0.0508 ± 0.0023	236.4 ± 4.9			
NZ_063	0.12	320	242	0.78	53.00 ± 1.16	0.0474 ± 0.0060	120.5 ± 2.6			
NZ_064	0.00	240	78	0.33	31.00 ± 0.62	0.0530 ± 0.0030	204.7 ± 4.1			
NZ_065	0.22	691	200	0.30	36.23 ± 0.52	0.0511 ± 0.0030	175.5 ± 2.5			

Table A1. Continued.

Labels	$^{206}Pb_c$ (1) (%)	U (ppm)	Th (ppm)	Th/U	$^{238}U/^{206}Pb^*$ (1)	$^{207}Pb^*/^{206}Pb^*$ (1)	$^{238}U/^{206}Pb^*$ age (1) (Ma)	$^{207}Pb^*/^{206}Pb^*$ age (1) (Ma)	Disc (2) (%)	Remarks
NZ_066	0.33	187	103	0.56	34.26 ± 0.66	0.0478 ± 0.0061	185.5 ± 3.5			
NZ_067	0.03	440	167	0.39	34.83 ± 0.61	0.0508 ± 0.0034	182.5 ± 3.1			
NZ_068	0.00	1057	224	0.22	3.25 ± 0.04	0.1124 ± 0.0011	1729.8 ± 18.1	1840 ± 18	5.99	
NZ_069	0.00	129	94	0.75	27.03 ± 0.64	0.0558 ± 0.0039	234.1 ± 5.4			
NZ_070	0.00	95	82	0.89	30.08 ± 0.78	0.0453 ± 0.0039	210.8 ± 5.4			
NZ_071	0.22	350	53	0.16	2.98 ± 0.04	0.1255 ± 0.0015	1864.1 ± 19.7	2037 ± 22	8.49	
NZ_072	0.00	68	86	1.30	28.78 ± 0.86	0.0430 ± 0.0047	220.2 ± 6.5			
NZ_073	0.00	216	90	0.43	3.02 ± 0.03	0.1168 ± 0.0017	1843.3 ± 18.2	1908 ± 26	3.39	
NZ_074	0.00	133	70	0.54	34.19 ± 0.90	0.0636 ± 0.0046	185.8 ± 4.8			discordant
NZ_075	0.75	251	233	0.95	59.77 ± 1.43	0.0454 ± 0.0096	107.0 ± 2.5			
NZ_076	0.00	205	178	0.89	28.80 ± 0.57	0.0493 ± 0.0028	220.1 ± 4.3			
NZ_077	0.00	47	29	0.63	30.14 ± 0.95	0.0506 ± 0.0063	210.4 ± 6.5			
NZ_078	0.00	1430	400	0.29	28.76 ± 0.34	0.0495 ± 0.0010	220.4 ± 2.6			
NZ_079	0.00	785	311	0.41	37.33 ± 0.48	0.0505 ± 0.0019	170.4 ± 2.2			
NZ_080	0.00	222	162	0.75	32.40 ± 0.66	0.0466 ± 0.0029	195.9 ± 3.9			
NZ_081	0.39	411	442	1.10	35.61 ± 0.66	0.0492 ± 0.0061	178.6 ± 3.3			
NZ_082	0.00	513	215	0.43	3.34 ± 0.04	0.1135 ± 0.0014	1686.2 ± 16.1	1857 ± 21	9.20	
NZ_083	0.17	356	170	0.49	2.83 ± 0.04	0.1391 ± 0.0018	1948.3 ± 25.9	2217 ± 22	12.12	
NZ_084	0.00	237	77	0.33	25.71 ± 0.46	0.0541 ± 0.0032	246.0 ± 4.3			
NZ_085	0.05	317	69	0.22	3.85 ± 0.05	0.1159 ± 0.0017	1487.1 ± 16.6	1894 ± 27	21.49	discordant
NZ_086	0.04	207	61	0.30	3.41 ± 0.04	0.1192 ± 0.0022	1657.5 ± 18.5	1946 ± 32	14.82	
NZ_087	0.00	83	42	0.52	35.07 ± 1.14	0.0495 ± 0.0056	181.3 ± 5.8			
NZ_088	0.00	1278	801	0.64	24.20 ± 0.26	0.0503 ± 0.0013	261.1 ± 2.8			
NZ_089	0.00	656	358	0.56	35.95 ± 0.53	0.0518 ± 0.0018	176.9 ± 2.6			
NZ_090	0.00	282	73	0.27	3.22 ± 0.04	0.1133 ± 0.0014	1744.1 ± 16.9	1854 ± 22	5.93	
NZ_091	0.30	187	79	0.43	33.15 ± 0.82	0.0500 ± 0.0050	191.6 ± 4.7			
NZ_092	0.00	746	362	0.50	33.39 ± 0.47	0.0509 ± 0.0018	190.2 ± 2.6			
NZ_093	0.00	74	57	0.80	28.75 ± 0.91	0.0528 ± 0.0054	220.4 ± 6.8			
NZ_094	0.22	1533	835	0.56	29.95 ± 0.36	0.0511 ± 0.0022	211.7 ± 2.5			
NZ_095	0.19	822	175	0.22	33.81 ± 0.44	0.0493 ± 0.0023	187.9 ± 2.4			
NZ_096	0.00	55	29	0.54	31.27 ± 1.06	0.0618 ± 0.0065	202.9 ± 6.8			
NZ_097	0.15	199	132	0.68	33.20 ± 0.75	0.0422 ± 0.0064	191.3 ± 4.3			
NZ_098	0.00	1170	308	0.27	25.55 ± 0.30	0.0508 ± 0.0011	247.5 ± 2.8			
NZ_099	1.70	630	275	0.45	34.93 ± 0.54	0.0489 ± 0.0040	182.0 ± 2.8			
NZ_100	0.00	994	95	0.10	3.59 ± 0.04	0.1120 ± 0.0012	1582.8 ± 15.2	1833 ± 19	13.65	
NZ_101	0.00	111	74	0.68	60.27 ± 2.02	0.0400 ± 0.0057	106.1 ± 3.5			
NZ_102	0.00	348	165	0.49	2.98 ± 0.05	0.1131 ± 0.0012	1864.7 ± 25.7	1851 ± 20	−0.74	
NZ_103	0.00	282	113	0.41	32.84 ± 0.58	0.0452 ± 0.0027	193.4 ± 3.3			
NZ_104	0.11	252	196	0.80	34.05 ± 0.68	0.0452 ± 0.0066	186.6 ± 3.7			
NZ_105	0.00	74	40	0.56	30.08 ± 0.94	0.0437 ± 0.0050	210.8 ± 6.5			
NZ_106	0.81	313	189	0.62	34.82 ± 0.75	0.0397 ± 0.0055	182.5 ± 3.9			
NZ_107	0.00	257	55	0.22	35.06 ± 0.71	0.0471 ± 0.0028	181.3 ± 3.6			
NZ_108	0.00	234	56	0.25	3.11 ± 0.04	0.1159 ± 0.0018	1798.9 ± 20.2	1895 ± 28	5.07	
NZ_109	1.40	95	106	1.14	31.30 ± 1.04	0.0475 ± 0.0149	202.7 ± 6.6			
NZ_110	0.00	425	594	1.43	15.36 ± 0.20	0.0579 ± 0.0017	406.7 ± 5.2			
NZ_111	0.00	551	227	0.42	30.94 ± 0.47	0.0502 ± 0.0018	205.0 ± 3.1			
NZ_112	0.00	119	17	0.14	35.22 ± 1.01	0.0572 ± 0.0043	180.5 ± 5.1			
NZ_113	0.04	719	22	0.03	3.63 ± 0.04	0.1278 ± 0.0012	1569.3 ± 16.1	2069 ± 16	24.15	discordant
NZ_114	0.00	322	209	0.67	35.53 ± 0.65	0.0453 ± 0.0022	178.9 ± 3.2			
NZ_115	0.20	309	36	0.12	27.04 ± 0.45	0.0513 ± 0.0030	234.1 ± 3.8			
NZ_116	0.00	195	64	0.34	3.90 ± 0.05	0.1113 ± 0.0018	1470.8 ± 17.1	1821 ± 30	19.23	discordant
NZ_117	0.06	228	125	0.56	3.21 ± 0.04	0.1165 ± 0.0021	1746.9 ± 20.3	1904 ± 32	8.25	
NZ_118	0.00	302	130	0.44	34.19 ± 0.56	0.0514 ± 0.0029	185.8 ± 3.0			
NZ_119	0.00	269	213	0.81	3.12 ± 0.04	0.1135 ± 0.0014	1789.7 ± 19.8	1857 ± 21	3.62	
NZ_120	0.00	226	118	0.54	26.03 ± 0.50	0.0499 ± 0.0025	243.0 ± 4.6			
NZ_121	0.00	496	504	1.04	29.63 ± 0.48	0.0521 ± 0.0018	214.0 ± 3.4			
NZ_122	0.02	105	59	0.58	2.63 ± 0.04	0.1544 ± 0.0034	2079.7 ± 29.1	2396 ± 37	13.20	
NZ_123	0.96	87	75	0.88	58.17 ± 2.20	0.0473 ± 0.0149	109.9 ± 4.1			
NZ_124	0.01	136	97	0.73	34.86 ± 0.81	0.0537 ± 0.0086	182.3 ± 4.2			
NZ_125	0.03	452	150	0.34	3.67 ± 0.06	0.1113 ± 0.0018	1553.9 ± 23.4	1822 ± 29	14.72	
NZ_126	0.01	388	195	0.52	35.53 ± 0.66	0.0484 ± 0.0041	178.9 ± 3.3			
NZ_127	1.20	315	447	1.45	68.60 ± 2.00	0.0416 ± 0.0117	93.3 ± 2.7			
NZ_128	0.28	513	134	0.27	3.19 ± 0.04	0.1207 ± 0.0024	1755.8 ± 19.7	1967 ± 35	10.74	
NZ_129	0.00	127	83	0.67	3.09 ± 0.05	0.1144 ± 0.0024	1805.2 ± 23.3	1871 ± 38	3.52	
NZ_130	0.46	131	63	0.50	36.25 ± 1.00	0.0451 ± 0.0070	175.4 ± 4.8			

Table A1. Continued.

Labels	$^{206}Pb_c$ (1) (%)	U (ppm)	Th (ppm)	Th/U	$^{238}U/^{206}Pb^*$ (1)	$^{207}Pb^*/^{206}Pb^*$ (1)	$^{238}U/^{206}Pb^*$ age (1) (Ma)	$^{207}Pb^*/^{206}Pb^*$ age (1) (Ma)	Disc (2) (%)	Remarks
NZ_131	0.00	168	101	0.62	35.68 ± 0.78	0.0432 ± 0.0035	178.2 ± 3.9			
NZ_132	0.00	121	72	0.61	26.32 ± 0.53	0.0520 ± 0.0038	240.4 ± 4.8			
NZ_133	0.00	278	133	0.49	30.78 ± 0.54	0.0467 ± 0.0025	206.1 ± 3.6			
NZ_134	0.08	463	74	0.16	2.99 ± 0.04	0.1124 ± 0.0017	1860.2 ± 22.1	1839 ± 28	− 1.15	
NZ_135	0.00	433	239	0.56	30.68 ± 0.59	0.0518 ± 0.0040	206.7 ± 3.9			
NZ_136	0.00	268	84	0.32	3.16 ± 0.05	0.1161 ± 0.0015	1773.7 ± 22.8	1898 ± 23	6.55	
NZ_137	0.64	113	76	0.69	29.78 ± 0.86	0.0496 ± 0.0084	212.9 ± 6.0			
NZ_138	0.00	117	164	1.45	40.98 ± 1.07	0.0527 ± 0.0047	155.4 ± 4.0			
NZ_139	0.00	302	95	0.32	24.07 ± 0.46	0.0510 ± 0.0022	262.4 ± 5.0			
NZ_140	0.00	97	46	0.48	30.82 ± 0.95	0.0504 ± 0.0049	205.8 ± 6.2			
NZ_141	0.66	56	33	0.61	33.65 ± 1.19	0.0634 ± 0.0115	188.8 ± 6.6			
NZ_142	0.21	517	104	0.21	2.63 ± 0.03	0.1596 ± 0.0022	2075.9 ± 20.4	2453 ± 22	15.37	discordant
NZ_143	0.00	88	77	0.90	34.03 ± 1.03	0.0445 ± 0.0047	186.7 ± 5.6			
NZ_144	0.45	212	107	0.52	33.93 ± 0.71	0.0449 ± 0.0056	187.3 ± 3.9			
NZ_145	1.35	145	132	0.94	37.51 ± 1.00	0.0401 ± 0.0099	169.6 ± 4.5			
NZ_146	0.00	93	61	0.67	29.26 ± 0.83	0.0481 ± 0.0040	216.7 ± 6.0			
YK_001	0.00	269	163	0.62	34.85 ± 0.57	0.0508 ± 0.0024	182.4 ± 2.9			
YK_002	0.22	649	118	0.19	26.82 ± 0.36	0.0480 ± 0.0018	236.0 ± 3.1			
YK_003	0.00	778	404	0.53	35.11 ± 0.38	0.0517 ± 0.0013	181.1 ± 2.0			
YK_004	0.00	333	151	0.47	2.42 ± 0.03	0.1527 ± 0.0016	2229.4 ± 23.3	2378 ± 17	6.25	
YK_005	0.00	312	237	0.78	2.63 ± 0.03	0.1390 ± 0.0013	2074.2 ± 21.4	2215 ± 16	6.36	
YK_006	0.00	245	1	0.01	2.80 ± 0.03	0.1231 ± 0.0015	1967.8 ± 18.4	2003 ± 22	1.76	
YK_007	0.00	235	102	0.45	23.75 ± 0.35	0.0551 ± 0.0023	265.9 ± 3.8			
YK_008	0.00	203	143	0.72	2.69 ± 0.03	0.1395 ± 0.0016	2035.7 ± 22.2	2222 ± 20	8.38	
YK_009	0.19	435	66	0.16	3.26 ± 0.04	0.1155 ± 0.0017	1726.0 ± 17.7	1889 ± 26	8.63	
YK_010	0.00	240	242	1.04	30.53 ± 0.67	0.0632 ± 0.0031	207.8 ± 4.5			discordant
YK_011	0.00	141	70	0.51	35.92 ± 0.80	0.0513 ± 0.0037	177.0 ± 3.9			
YK_012	0.64	141	82	0.59	29.93 ± 0.65	0.0469 ± 0.0061	211.9 ± 4.6			
YK_013	0.17	227	72	0.32	3.31 ± 0.04	0.1137 ± 0.0018	1703.8 ± 18.6	1860 ± 28	8.40	
YK_014	0.00	69	45	0.68	35.29 ± 0.91	0.0510 ± 0.0051	180.1 ± 4.6			
YK_015	0.30	83	20	0.25	29.43 ± 0.70	0.0576 ± 0.0051	215.4 ± 5.0			
YK_016	0.00	481	178	0.38	2.82 ± 0.04	0.1416 ± 0.0013	1957.4 ± 22.3	2248 ± 16	12.93	
YK_017	0.00	281	148	0.54	30.46 ± 0.49	0.0538 ± 0.0024	208.2 ± 3.3			
YK_018	0.00	463	263	0.58	38.75 ± 0.65	0.0474 ± 0.0020	164.2 ± 2.7			
YK_019	0.00	264	133	0.52	25.34 ± 0.43	0.0523 ± 0.0020	249.5 ± 4.1			
YK_020	0.29	269	89	0.34	33.71 ± 0.68	0.0497 ± 0.0041	188.4 ± 3.8			
YK_021	0.04	74	46	0.63	35.04 ± 1.11	0.0557 ± 0.0103	181.4 ± 5.7			
YK_022	0.06	309	151	0.50	29.53 ± 0.48	0.0492 ± 0.0038	214.7 ± 3.4			
YK_023	0.00	92	103	1.16	3.05 ± 0.04	0.1137 ± 0.0019	1829.3 ± 21.4	1861 ± 29	1.70	
YK_024	0.00	65	44	0.70	26.92 ± 0.74	0.0427 ± 0.0048	235.2 ± 6.4			
YK_025	0.05	378	86	0.23	28.20 ± 0.44	0.0545 ± 0.0028	224.7 ± 3.5			
YK_026	0.00	628	333	0.54	3.08 ± 0.03	0.1280 ± 0.0011	1810.5 ± 16.9	2072 ± 15	12.62	
YK_027	0.37	41	12	0.30	24.77 ± 0.79	0.0372 ± 0.0085	255.1 ± 8.0			
YK_028	0.00	319	133	0.43	31.09 ± 0.48	0.0498 ± 0.0026	204.1 ± 3.1			
YK_029	0.02	829	430	0.53	29.75 ± 0.41	0.0515 ± 0.0026	213.1 ± 2.9			
YK_030	0.93	153	78	0.52	34.82 ± 0.70	0.0445 ± 0.0061	182.5 ± 3.6			
YK_031	0.00	174	87	0.51	57.26 ± 1.42	0.0480 ± 0.0042	111.6 ± 2.7			
YK_032	0.09	250	129	0.53	31.42 ± 0.68	0.0481 ± 0.0045	202.0 ± 4.3			
YK_033	0.00	605	21	0.03	26.09 ± 0.33	0.0490 ± 0.0017	242.5 ± 3.0			
YK_034	0.07	622	278	0.46	32.50 ± 0.50	0.0502 ± 0.0031	195.4 ± 3.0			
YK_035	0.00	1370	437	0.33	24.91 ± 0.27	0.0528 ± 0.0011	253.7 ± 2.7			
YK_036	0.15	185	104	0.58	27.96 ± 0.61	0.0499 ± 0.0050	226.6 ± 4.8			
YK_037	0.23	528	97	0.19	2.99 ± 0.03	0.1309 ± 0.0018	1859.6 ± 18.9	2111 ± 23	11.91	
YK_038	0.72	317	187	0.61	34.16 ± 0.52	0.0481 ± 0.0047	186.0 ± 2.8			
YK_039	0.16	238	81	0.35	33.52 ± 0.62	0.0506 ± 0.0040	189.5 ± 3.4			
YK_040	0.00	384	472	1.26	66.76 ± 1.32	0.0508 ± 0.0034	95.8 ± 1.9			
YK_041	0.00	262	47	0.18	34.72 ± 0.59	0.0480 ± 0.0024	183.1 ± 3.1			
YK_042	0.00	392	397	1.04	32.24 ± 0.43	0.0520 ± 0.0022	196.9 ± 2.6			
YK_043	0.28	517	244	0.48	13.27 ± 0.19	0.0530 ± 0.0024	468.4 ± 6.4			
YK_044	0.00	803	128	0.16	24.60 ± 0.34	0.0519 ± 0.0013	256.8 ± 3.5			
YK_045	0.00	374	180	0.49	34.06 ± 0.55	0.0493 ± 0.0020	186.5 ± 3.0			
YK_046	0.16	597	48	0.08	3.15 ± 0.03	0.1161 ± 0.0013	1779.2 ± 14.6	1898 ± 20	6.26	
YK_047	0.00	118	104	0.90	32.72 ± 0.82	0.0613 ± 0.0047	194.1 ± 4.8			discordant
YK_048	0.00	222	59	0.27	3.39 ± 0.05	0.1127 ± 0.0018	1664.9 ± 20.3	1845 ± 30	9.76	
YK_049	0.00	133	63	0.49	32.41 ± 0.72	0.0470 ± 0.0032	195.9 ± 4.3			

Table A1. Continued.

Labels	$^{206}Pb_c$ (1) (%)	U (ppm)	Th (ppm)	Th/U	$^{238}U/^{206}Pb^{*(1)}$	$^{207}Pb^{*}/^{206}Pb^{*(1)}$	$^{238}U/^{206}Pb^{*}$ age(1) (Ma)	$^{207}Pb^{*}/^{206}Pb^{*}$ age(1) (Ma)	Disc (2) (%)	Remarks
YK_050	0.00	88	49	0.57	28.80 ± 0.67	0.0496 ± 0.0044	220.0 ± 5.1			
YK_051	0.00	251	167	0.68	31.57 ± 0.59	0.0523 ± 0.0028	201.0 ± 3.7			
YK_052	0.00	152	87	0.59	32.23 ± 0.70	0.0463 ± 0.0033	197.0 ± 4.2			
YK_053	0.00	70	46	0.68	32.80 ± 0.81	0.0532 ± 0.0055	193.6 ± 4.7			
YK_054	0.16	78	38	0.50	21.23 ± 0.57	0.0564 ± 0.0071	296.7 ± 7.8			
YK_055	0.00	138	64	0.48	26.60 ± 0.52	0.0454 ± 0.0033	237.9 ± 4.6			
YK_056	0.00	383	27	0.07	4.04 ± 0.05	0.1132 ± 0.0016	1424.8 ± 16.3	1852 ± 25	23.07	discordant
YK_057	0.00	323	58	0.18	3.73 ± 0.04	0.1186 ± 0.0014	1530.0 ± 15.3	1936 ± 21	20.97	discordant
YK_058	0.00	210	107	0.52	33.77 ± 0.62	0.0495 ± 0.0030	188.1 ± 3.4			
YK_059	1.31	60	16	0.27	28.33 ± 0.93	0.0653 ± 0.0097	223.6 ± 7.2			
YK_060	0.00	114	58	0.52	2.72 ± 0.03	0.1307 ± 0.0020	2019.0 ± 21.4	2109 ± 26	4.27	
YK_061	0.25	448	364	0.83	34.96 ± 0.58	0.0480 ± 0.0038	181.8 ± 3.0			
YK_062	0.08	380	310	0.84	14.48 ± 0.19	0.0560 ± 0.0030	430.4 ± 5.6			
YK_063	0.00	59	37	0.65	29.46 ± 0.81	0.0539 ± 0.0052	215.2 ± 5.8			
YK_064	0.04	458	46	0.10	3.47 ± 0.04	0.1140 ± 0.0012	1633.9 ± 15.1	1865 ± 20	12.39	
YK_065	0.00	217	109	0.52	36.82 ± 0.66	0.0536 ± 0.0030	172.7 ± 3.0			
YK_066	0.00	676	371	0.56	34.84 ± 0.49	0.0482 ± 0.0017	182.4 ± 2.6			
YK_067	0.06	362	33	0.09	2.65 ± 0.03	0.1553 ± 0.0016	2061.3 ± 21.9	2406 ± 18	14.33	
YK_068	0.00	409	36	0.09	29.29 ± 0.40	0.0504 ± 0.0020	216.4 ± 2.9			
YK_069	0.00	220	79	0.37	15.91 ± 0.27	0.0850 ± 0.0026	393.0 ± 6.5	1317 ± 59	70.16	discordant
YK_070	0.00	1260	563	0.46	18.18 ± 0.23	0.0540 ± 0.0009	345.2 ± 4.3			
YK_071	0.00	232	151	0.67	30.11 ± 0.48	0.0486 ± 0.0024	210.6 ± 3.3			
YK_072	0.16	257	128	0.51	35.75 ± 0.67	0.0477 ± 0.0046	177.8 ± 3.3			
YK_073	1.59	570	391	0.70	29.57 ± 0.48	0.0554 ± 0.0050	214.4 ± 3.4			
YK_074	0.00	882	234	0.27	40.23 ± 0.51	0.0478 ± 0.0017	158.3 ± 2.0			
YK_075	0.24	169	101	0.61	67.98 ± 1.84	0.0683 ± 0.0088	94.1 ± 2.5			discordant
YK_076	0.00	205	134	0.67	34.63 ± 0.70	0.0505 ± 0.0028	183.5 ± 3.6			
YK_077	0.00	812	624	0.79	30.19 ± 0.41	0.0485 ± 0.0013	210.0 ± 2.8			
YK_078	0.00	181	25	0.14	28.90 ± 0.52	0.0521 ± 0.0031	219.3 ± 3.9			
YK_079	0.23	89	78	0.89	30.82 ± 0.83	0.0536 ± 0.0091	205.8 ± 5.5			
YK_080	0.36	1170	479	0.42	29.91 ± 0.39	0.0480 ± 0.0020	212.0 ± 2.7			
YK_081	0.13	412	297	0.74	29.84 ± 0.50	0.0473 ± 0.0040	212.5 ± 3.5			
YK_082	0.00	369	158	0.44	34.81 ± 0.49	0.0483 ± 0.0022	182.6 ± 2.5			
YK_083	0.00	781	401	0.53	34.57 ± 0.47	0.0485 ± 0.0015	183.8 ± 2.5			
YK_084	0.00	117	64	0.56	35.20 ± 0.82	0.0484 ± 0.0043	180.6 ± 4.2			
YK_085	0.00	176	65	0.38	3.65 ± 0.05	0.1105 ± 0.0021	1560.7 ± 20.5	1808 ± 35	13.68	
YK_086	0.16	142	96	0.69	34.08 ± 0.75	0.0498 ± 0.0064	186.4 ± 4.0			
YK_087	0.00	177	54	0.31	3.19 ± 0.04	0.1135 ± 0.0018	1758.2 ± 21.1	1857 ± 28	5.32	
YK_088	0.00	976	16	0.02	3.36 ± 0.03	0.1115 ± 0.0010	1678.6 ± 14.8	1824 ± 17	7.97	
YK_089	0.00	1137	436	0.39	32.44 ± 0.34	0.0515 ± 0.0013	195.7 ± 2.0			
YK_090	0.00	245	320	1.34	50.72 ± 0.97	0.0471 ± 0.0034	125.9 ± 2.4			
YK_091	0.00	86	55	0.66	26.30 ± 0.65	0.0503 ± 0.0043	240.6 ± 5.8			
YK_092	0.00	59	45	0.77	11.88 ± 0.29	0.0505 ± 0.0039	520.9 ± 12.2			
YK_093	0.00	131	101	0.79	28.65 ± 0.63	0.0471 ± 0.0036	221.2 ± 4.8			
YK_094	0.39	199	144	0.74	33.16 ± 0.73	0.0434 ± 0.0060	191.5 ± 4.2			
YK_095	0.00	719	448	0.64	28.55 ± 0.34	0.0525 ± 0.0017	222.0 ± 2.6			
YK_096	0.00	227	188	0.85	27.84 ± 0.53	0.0495 ± 0.0028	227.5 ± 4.2			
YK_097	0.00	245	65	0.27	35.85 ± 0.66	0.0529 ± 0.0030	177.3 ± 3.2			
YK_098	0.34	170	107	0.65	34.66 ± 0.76	0.0488 ± 0.0065	183.3 ± 4.0			
YK_099	0.76	196	121	0.63	2.69 ± 0.03	0.1218 ± 0.0030	2040.0 ± 21.3	1984 ± 42	− 2.82	
YK_100	0.25	181	50	0.28	3.81 ± 0.06	0.1252 ± 0.0030	1500.9 ± 22.2	2033 ± 41	26.18	discordant
YK_101	0.00	251	183	0.75	32.86 ± 0.62	0.0522 ± 0.0030	193.3 ± 3.6			
YK_102	0.00	1144	83	0.07	3.35 ± 0.04	0.1136 ± 0.0011	1684.4 ± 16.5	1858 ± 17	9.34	
YK_103	0.00	343	235	0.70	23.52 ± 0.39	0.0505 ± 0.0018	268.5 ± 4.4			
YK_104	0.00	31	52	1.70	36.31 ± 1.41	0.0560 ± 0.0100	175.1 ± 6.7			
YK_105	0.10	227	85	0.38	3.64 ± 0.05	0.1128 ± 0.0021	1565.4 ± 17.7	1847 ± 33	15.25	discordant
YK_106	0.00	542	293	0.55	2.45 ± 0.03	0.1734 ± 0.0015	2203.9 ± 21.3	2592 ± 15	14.97	
YK_107	0.56	626	537	0.88	31.65 ± 0.49	0.0565 ± 0.0033	200.5 ± 3.0			
YK_108	0.00	990	1387	1.44	29.24 ± 0.33	0.0504 ± 0.0011	216.8 ± 2.4			
YK_109	0.45	147	107	0.75	34.62 ± 0.74	0.0458 ± 0.0065	183.6 ± 3.9			
YK_110	0.00	319	136	0.44	33.90 ± 0.57	0.0445 ± 0.0034	187.4 ± 3.1			
YK_111	0.00	831	134	0.17	34.73 ± 0.43	0.0519 ± 0.0015	183.0 ± 2.2			
YK_112	0.00	866	696	0.82	29.49 ± 0.40	0.0544 ± 0.0013	215.0 ± 2.9			discordant
YK_113	0.13	205	65	0.32	28.32 ± 0.52	0.0554 ± 0.0038	223.7 ± 4.0			
YK_114	0.00	710	220	0.32	26.42 ± 0.35	0.0498 ± 0.0013	239.5 ± 3.1			

Table A1. Continued.

Labels	$^{206}Pb_c$ (1) (%)	U (ppm)	Th (ppm)	Th/U	$^{238}U/^{206}Pb^{*(1)}$	$^{207}Pb^{*}/^{206}Pb^{*(1)}$	$^{238}U/^{206}Pb^{*}$ age(1) (Ma)	$^{207}Pb^{*}/^{206}Pb^{*}$ age(1) (Ma)	Disc (2) (%)	Remarks
YK_115	0.00	326	115	0.36	2.42 ± 0.03	0.1209 ± 0.0013	2226.5 ± 25.7	1970 ± 19	− 13.02	
YK_116	0.37	95	59	0.64	25.12 ± 0.61	0.0428 ± 0.0070	251.6 ± 6.0			
YK_117	0.00	153	107	0.72	24.03 ± 0.48	0.0521 ± 0.0028	262.9 ± 5.2			
YK_118	0.00	234	82	0.36	30.66 ± 0.57	0.0464 ± 0.0024	206.9 ± 3.8			
YK_119	0.00	112	79	0.72	2.50 ± 0.03	0.1489 ± 0.0024	2167.3 ± 25.2	2335 ± 27	7.18	
YK_120	0.10	389	276	0.73	27.84 ± 0.43	0.0555 ± 0.0040	227.5 ± 3.5			
YK_121	0.00	179	189	1.08	3.82 ± 0.06	0.1145 ± 0.0019	1499.7 ± 21.5	1874 ± 29	19.98	discordant
YK_122	0.00	210	110	0.54	2.82 ± 0.03	0.1437 ± 0.0019	1958.8 ± 19.8	2274 ± 22	13.86	
YK_123	0.62	298	169	0.58	30.45 ± 0.57	0.0523 ± 0.0040	208.3 ± 3.9			
YK_124	0.00	105	89	0.87	32.44 ± 0.79	0.0524 ± 0.0046	195.7 ± 4.7			
YK_125	0.13	298	177	0.61	34.34 ± 0.66	0.0517 ± 0.0048	185.0 ± 3.5			
YK_126	0.61	43	25	0.60	26.64 ± 1.22	0.0634 ± 0.0131	237.6 ± 10.7			
YK_127	0.14	631	76	0.12	35.89 ± 0.54	0.0473 ± 0.0022	177.2 ± 2.6			
YK_128	0.00	361	175	0.50	3.02 ± 0.03	0.1221 ± 0.0015	1846.2 ± 16.0	1988 ± 22	7.13	
YK_129	0.00	53	36	0.71	3.65 ± 0.06	0.1084 ± 0.0025	1560.7 ± 21.1	1773 ± 42	11.97	
YK_130	0.04	365	158	0.44	36.00 ± 0.58	0.0510 ± 0.0044	176.6 ± 2.8			
YK_131	0.00	29	9	0.30	17.62 ± 0.65	0.0518 ± 0.0058	355.9 ± 12.9			
YK_132	0.30	146	81	0.57	33.06 ± 0.79	0.0498 ± 0.0049	192.1 ± 4.5			
YK_133	0.00	250	104	0.42	5.46 ± 0.08	0.1249 ± 0.0020	1084.4 ± 15.5	2029 ± 27	46.55	discordant
YK_134	0.00	1172	138	0.12	27.82 ± 0.30	0.0515 ± 0.0012	227.6 ± 2.4			
YK_135	0.21	474	70	0.15	3.60 ± 0.04	0.1104 ± 0.0016	1580.8 ± 14.1	1807 ± 26	12.52	
YK_136	0.00	163	88	0.55	34.32 ± 0.69	0.0508 ± 0.0029	185.2 ± 3.7			
YK_137	0.00	863	389	0.46	31.20 ± 0.36	0.0504 ± 0.0015	203.4 ± 2.3			
YK_138	0.00	289	93	0.33	3.13 ± 0.04	0.1120 ± 0.0018	1786.6 ± 18.1	1834 ± 28	2.58	
YK_139	0.27	462	858	1.91	56.30 ± 1.23	0.0454 ± 0.0113	113.5 ± 2.5			
YK_140	0.95	1480	288	0.20	22.00 ± 0.26	0.0467 ± 0.0014	286.6 ± 3.3			discordant
YK_141	0.49	345	95	0.28	34.19 ± 0.57	0.0486 ± 0.0034	185.9 ± 3.1			
YK_142	0.02	1016	233	0.23	3.02 ± 0.03	0.1233 ± 0.0010	1842.0 ± 16.9	2006 ± 15	8.17	
YK_143	0.13	770	422	0.56	30.10 ± 0.40	0.0519 ± 0.0025	210.7 ± 2.8			
YK_144	0.24	465	401	0.88	22.80 ± 0.31	0.0531 ± 0.0037	276.7 ± 3.7			
YK_145	0.22	528	306	0.59	31.81 ± 0.48	0.0501 ± 0.0034	199.5 ± 2.9			
SK_001	0.00	379	36	0.10	3.63 ± 0.04	0.1127 ± 0.0013	1570.3 ± 16.8	1844 ± 21	14.84	
SK_002	0.54	390	218	0.57	34.26 ± 0.54	0.0500 ± 0.0041	185.5 ± 2.9			
SK_003	0.00	381	230	0.62	34.00 ± 0.54	0.0498 ± 0.0023	186.9 ± 2.9			
SK_004	0.00	185	119	0.66	59.70 ± 1.52	0.0456 ± 0.0034	107.1 ± 2.7			
SK_005	0.27	1458	253	0.18	2.92 ± 0.03	0.1233 ± 0.0014	1896.8 ± 19.6	2005 ± 21	5.40	
SK_006	0.60	191	104	0.56	32.72 ± 0.61	0.0467 ± 0.0056	194.1 ± 3.5			
SK_007	3.99	50	51	1.05	4.78 ± 0.09	0.0797 ± 0.0067	1225.0 ± 21.3	1192 ± 157	− 2.77	
SK_008	0.00	183	121	0.68	33.47 ± 0.76	0.0578 ± 0.0031	189.8 ± 4.3			discordant
SK_009	0.00	665	287	0.44	30.47 ± 0.44	0.0507 ± 0.0014	208.2 ± 3.0			
SK_010	0.30	454	197	0.45	36.51 ± 0.71	0.0487 ± 0.0033	174.2 ± 3.3			
SK_011	0.00	306	175	0.59	3.11 ± 0.04	0.1133 ± 0.0014	1796.2 ± 18.2	1854 ± 22	3.12	
SK_012	0.00	126	164	1.34	3.05 ± 0.04	0.1090 ± 0.0018	1827.4 ± 20.8	1783 ± 30	− 2.49	
SK_013	0.29	212	56	0.27	27.58 ± 0.52	0.0536 ± 0.0034	229.6 ± 4.3			
SK_014	1.92	1045	1049	1.03	22.98 ± 0.29	0.0396 ± 0.0033	274.6 ± 3.4			discordant
SK_015	0.00	129	86	0.68	26.84 ± 0.72	0.0492 ± 0.0041	235.8 ± 6.2			
SK_016	0.45	552	522	0.97	28.90 ± 0.45	0.0487 ± 0.0043	219.3 ± 3.4			
SK_017	1.87	71	22	0.32	41.00 ± 1.44	0.0338 ± 0.0096	155.3 ± 5.4			
SK_018	0.00	278	215	0.79	34.02 ± 0.66	0.0520 ± 0.0030	186.8 ± 3.6			
SK_019	0.89	197	100	0.52	33.97 ± 0.65	0.0442 ± 0.0062	187.0 ± 3.5			
SK_020	0.00	99	68	0.70	61.28 ± 1.94	0.0414 ± 0.0061	104.4 ± 3.3			
SK_021	0.08	1159	577	0.51	29.36 ± 0.44	0.0496 ± 0.0022	215.9 ± 3.2			
SK_022	0.19	301	159	0.54	34.06 ± 0.68	0.0436 ± 0.0045	186.5 ± 3.7			
SK_023	1.15	480	231	0.49	32.56 ± 0.70	0.0466 ± 0.0040	195.0 ± 4.1			
SK_024	0.22	239	149	0.64	29.19 ± 0.67	0.0491 ± 0.0048	217.2 ± 4.9			
SK_025	0.24	485	141	0.30	32.35 ± 0.70	0.0447 ± 0.0030	196.3 ± 4.2			
SK_026	0.20	354	144	0.42	31.26 ± 0.56	0.0503 ± 0.0034	203.0 ± 3.6			
SK_027	1.10	55	121	2.25	3.08 ± 0.07	0.0990 ± 0.0097	1811.2 ± 34.9	1606 ± 172	− 12.78	
SK_028	0.00	288	93	0.33	2.87 ± 0.04	0.1201 ± 0.0017	1927.0 ± 25.1	1959 ± 25	1.63	
SK_029	0.01	519	71	0.14	3.17 ± 0.04	0.1124 ± 0.0015	1766.1 ± 18.5	1839 ± 23	3.97	
SK_030	0.00	508	378	0.76	5.82 ± 0.09	0.1098 ± 0.0017	1022.7 ± 15.2	1798 ± 27	43.12	discordant
SK_031	0.32	229	178	0.80	34.95 ± 0.84	0.0464 ± 0.0069	181.9 ± 4.3			
SK_032	1.18	242	234	0.99	31.65 ± 0.62	0.0382 ± 0.0071	200.5 ± 3.8			
SK_033	0.35	244	210	0.88	3.10 ± 0.04	0.1083 ± 0.0026	1801.3 ± 20.5	1773 ± 43	− 1.60	
SK_034	0.00	2513	328	0.13	32.71 ± 0.44	0.0496 ± 0.0009	194.1 ± 2.6			

Table A1. Continued.

Labels	$^{206}Pb_c$ (1) (%)	U (ppm)	Th (ppm)	Th/U	$^{238}U/^{206}Pb^{*(1)}$	$^{207}Pb^{*}/^{206}Pb^{*(1)}$	$^{238}U/^{206}Pb^{*}$ age(1) (Ma)	$^{207}Pb^{*}/^{206}Pb^{*}$ age(1) (Ma)	Disc (2) (%)	Remarks
SK_035	0.21	247	166	0.69	29.18 ± 0.57	0.0533 ± 0.0061	217.2 ± 4.2			
SK_036	0.00	307	171	0.57	62.59 ± 1.50	0.0501 ± 0.0032	102.2 ± 2.4			
SK_037	0.00	520	373	0.74	32.20 ± 0.49	0.0488 ± 0.0021	197.1 ± 2.9			
SK_038	0.00	353	233	0.68	29.90 ± 0.53	0.0493 ± 0.0026	212.1 ± 3.7			
SK_039	0.00	111	68	0.63	32.04 ± 0.86	0.0519 ± 0.0046	198.1 ± 5.2			
SK_040	0.00	57	18	0.33	2.49 ± 0.04	0.1661 ± 0.0039	2176.4 ± 32.8	2520 ± 39	13.63	
SK_041	0.22	817	539	0.68	57.56 ± 0.90	0.0452 ± 0.0040	111.0 ± 1.7			
SK_042	0.76	278	150	0.55	45.21 ± 0.88	0.0467 ± 0.0060	141.0 ± 2.7			
SK_043	0.72	176	73	0.42	30.19 ± 0.75	0.0430 ± 0.0053	210.0 ± 5.2			
SK_044	0.09	927	76	0.08	3.06 ± 0.03	0.1185 ± 0.0013	1821.6 ± 17.9	1935 ± 19	5.86	
SK_045	0.00	116	69	0.61	33.07 ± 0.86	0.0575 ± 0.0040	192.0 ± 4.9			
SK_046	0.00	506	205	0.42	32.31 ± 0.52	0.0477 ± 0.0017	196.5 ± 3.1			
SK_047	0.03	388	30	0.08	3.17 ± 0.04	0.1140 ± 0.0013	1767.3 ± 19.4	1865 ± 21	5.24	
SK_048	0.26	245	52	0.22	3.50 ± 0.05	0.1089 ± 0.0022	1618.9 ± 21.2	1782 ± 36	9.15	
SK_049	0.39	109	56	0.52	34.11 ± 0.95	0.0446 ± 0.0070	186.3 ± 5.1			
SK_050	0.13	551	113	0.21	3.19 ± 0.04	0.1135 ± 0.0014	1759.1 ± 21.6	1857 ± 23	5.27	
SK_051	0.02	274	155	0.58	30.65 ± 0.60	0.0497 ± 0.0050	206.9 ± 4.0			
SK_052	0.00	223	98	0.45	33.84 ± 0.66	0.0545 ± 0.0031	187.7 ± 3.6			
SK_053	1.52	103	63	0.63	34.06 ± 0.98	0.0357 ± 0.0090	186.5 ± 5.3			
SK_054	0.60	535	412	0.79	34.65 ± 0.60	0.0477 ± 0.0041	183.4 ± 3.1			
SK_055	0.07	230	89	0.40	3.74 ± 0.05	0.1064 ± 0.0020	1527.1 ± 20.0	1740 ± 34	12.23	
SK_056	0.00	198	91	0.47	33.29 ± 0.66	0.0508 ± 0.0033	190.8 ± 3.7			
SK_057	0.00	203	133	0.67	32.87 ± 0.74	0.0491 ± 0.0030	193.2 ± 4.3			
SK_058	0.00	390	58	0.15	28.05 ± 0.48	0.0534 ± 0.0024	225.8 ± 3.8			
SK_059	1.02	398	403	1.04	28.91 ± 0.52	0.0443 ± 0.0056	219.2 ± 3.9			
SK_060	0.03	327	59	0.19	3.41 ± 0.05	0.1103 ± 0.0016	1656.4 ± 19.9	1805 ± 27	8.23	
SK_061	0.00	199	131	0.68	29.39 ± 0.60	0.0467 ± 0.0028	215.7 ± 4.3			
SK_062	1.02	136	89	0.67	34.81 ± 0.92	0.0483 ± 0.0086	182.6 ± 4.8			
SK_063	0.00	416	100	0.25	3.13 ± 0.04	0.1119 ± 0.0013	1787.6 ± 17.7	1831 ± 20	2.37	
SK_064	2.14	56	16	0.30	36.83 ± 1.54	0.0355 ± 0.0123	172.7 ± 7.1			
SK_065	0.00	116	75	0.67	29.86 ± 0.78	0.0433 ± 0.0039	212.3 ± 5.4			
SK_066	0.18	135	122	0.92	2.72 ± 0.04	0.1293 ± 0.0033	2016.8 ± 27.5	2089 ± 45	3.46	
SK_067	0.61	354	187	0.54	29.54 ± 0.62	0.0463 ± 0.0039	214.6 ± 4.4			
SK_068	0.15	298	113	0.39	24.98 ± 0.48	0.0497 ± 0.0039	253.0 ± 4.8			
SK_069	1.35	209	129	0.63	29.03 ± 0.63	0.0396 ± 0.0074	218.3 ± 4.6			
SK_070	0.00	124	58	0.48	33.57 ± 0.99	0.0501 ± 0.0042	189.2 ± 5.5			
SK_071	0.08	201	108	0.55	33.89 ± 0.84	0.0532 ± 0.0057	187.5 ± 4.6			
SK_072	0.00	257	146	0.58	33.06 ± 0.67	0.0497 ± 0.0034	192.1 ± 3.8			
SK_073	0.00	1482	835	0.58	32.60 ± 0.43	0.0599 ± 0.0013	194.8 ± 2.6			discordant
SK_074	0.72	178	128	0.74	62.66 ± 1.95	0.0549 ± 0.0100	102.1 ± 3.1			
SK_075	0.33	177	78	0.45	34.51 ± 0.89	0.0441 ± 0.0054	184.1 ± 4.7			
SK_076	0.05	844	114	0.14	2.94 ± 0.05	0.1177 ± 0.0014	1886.6 ± 25.8	1922 ± 21	1.84	
SK_077	0.00	463	35	0.08	3.55 ± 0.05	0.1135 ± 0.0015	1599.0 ± 21.3	1858 ± 24	13.94	
SK_078	0.00	659	248	0.39	29.86 ± 0.51	0.0501 ± 0.0016	212.3 ± 3.6			
SK_079	0.00	486	251	0.53	28.50 ± 0.53	0.0537 ± 0.0023	222.3 ± 4.1			
SK_080	0.24	157	84	0.55	22.46 ± 0.52	0.0529 ± 0.0057	280.9 ± 6.3			
SK_081	0.47	262	124	0.49	32.29 ± 0.65	0.0444 ± 0.0054	196.6 ± 3.9			
SK_082	0.34	975	369	0.39	18.59 ± 0.30	0.0503 ± 0.0022	337.8 ± 5.4			
SK_083	0.31	706	247	0.36	2.51 ± 0.03	0.1480 ± 0.0022	2158.1 ± 23.4	2324 ± 26	7.14	
SK_084	0.00	654	48	0.08	3.57 ± 0.06	0.1281 ± 0.0017	1592.5 ± 23.2	2073 ± 24	23.18	discordant
SK_085	0.13	231	109	0.48	55.34 ± 1.66	0.0530 ± 0.0072	115.5 ± 3.4			
SK_086	0.00	105	117	1.14	63.08 ± 2.52	0.0405 ± 0.0087	101.4 ± 4.0			
SK_087	0.97	340	162	0.49	3.07 ± 0.05	0.1144 ± 0.0025	1815.5 ± 23.6	1871 ± 39	2.97	
SK_088	0.40	232	136	0.60	28.01 ± 0.59	0.0520 ± 0.0051	226.1 ± 4.7			
SK_089	0.61	694	487	0.72	28.85 ± 0.49	0.0462 ± 0.0036	219.7 ± 3.6			
SK_090	0.00	485	310	0.65	33.21 ± 0.65	0.0503 ± 0.0022	191.3 ± 3.7			
SK_091	0.00	505	158	0.32	4.06 ± 0.06	0.1128 ± 0.0016	1418.0 ± 17.2	1846 ± 25	23.18	discordant
SK_092	0.00	81	10	0.12	26.87 ± 0.83	0.0491 ± 0.0050	235.6 ± 7.2			
SK_093	0.00	299	61	0.21	3.29 ± 0.05	0.1130 ± 0.0017	1711.2 ± 22.1	1849 ± 26	7.45	
SK_094	0.00	671	72	0.11	35.06 ± 0.46	0.0500 ± 0.0017	181.3 ± 2.4			
SK_095	0.00	213	82	0.39	30.78 ± 0.59	0.0547 ± 0.0030	206.1 ± 3.9			
SK_096	0.00	72	43	0.61	64.13 ± 2.73	0.0418 ± 0.0081	99.7 ± 4.2			
SK_097	0.00	388	235	0.62	2.82 ± 0.04	0.1229 ± 0.0015	1958.3 ± 22.5	2000 ± 22	2.08	
SK_098	0.00	688	12	0.02	3.37 ± 0.04	0.1111 ± 0.0014	1676.6 ± 18.1	1819 ± 22	7.83	
SK_099	0.00	983	648	0.68	29.86 ± 0.47	0.0508 ± 0.0015	212.3 ± 3.3			

Table A1. Continued.

Labels	$^{206}Pb_c$ (1) (%)	U (ppm)	Th (ppm)	Th/U	$^{238}U/^{206}Pb^{*}$ (1)	$^{207}Pb^{*}/^{206}Pb^{*}$ (1)	$^{238}U/^{206}Pb^{*}$ age (1) (Ma)	$^{207}Pb^{*}/^{206}Pb^{*}$ age (1) (Ma)	Disc (2) (%)	Remarks
SK_100	0.72	553	263	0.49	36.49 ± 0.63	0.0482 ± 0.0040	174.3 ± 2.9			
SK_101	0.04	219	58	0.27	3.16 ± 0.05	0.1126 ± 0.0020	1770.6 ± 22.2	1843 ± 33	3.93	
SK_102	0.00	138	95	0.71	57.56 ± 1.87	0.0412 ± 0.0046	111.0 ± 3.6			
SK_103	0.00	173	65	0.38	30.32 ± 0.65	0.0449 ± 0.0029	209.2 ± 4.4			
SK_104	0.00	222	110	0.51	31.87 ± 0.67	0.0477 ± 0.0026	199.2 ± 4.1			
SK_105	0.07	155	73	0.48	24.75 ± 0.47	0.0518 ± 0.0051	255.4 ± 4.8			
SK_106	0.14	130	52	0.41	36.61 ± 0.98	0.0419 ± 0.0055	173.7 ± 4.6			
SK_107	0.00	276	41	0.15	3.23 ± 0.04	0.1132 ± 0.0016	1738.9 ± 20.0	1852 ± 25	6.11	
SK_108	0.55	221	135	0.62	30.22 ± 0.64	0.0424 ± 0.0060	209.9 ± 4.3			
SK_109	0.00	598	302	0.52	2.77 ± 0.04	0.1235 ± 0.0015	1987.1 ± 25.9	2008 ± 22	1.04	
SK_110	0.00	90	48	0.55	32.84 ± 1.04	0.0487 ± 0.0054	193.4 ± 6.0			
SK_111	0.00	514	334	0.67	2.26 ± 0.03	0.1583 ± 0.0019	2358.0 ± 23.4	2439 ± 20	3.32	
SK_112	0.00	168	60	0.36	3.02 ± 0.05	0.1143 ± 0.0020	1843.7 ± 24.2	1870 ± 31	1.41	
SK_113	0.10	541	378	0.72	27.50 ± 0.43	0.0570 ± 0.0040	230.3 ± 3.6			
SK_114	0.26	158	140	0.90	30.98 ± 0.77	0.0464 ± 0.0084	204.8 ± 5.0			
SK_115	0.00	1917	668	0.36	27.56 ± 0.38	0.0500 ± 0.0010	229.7 ± 3.1			
SK_116	0.00	320	228	0.73	33.53 ± 0.63	0.0488 ± 0.0023	189.5 ± 3.5			
SK_117	0.00	1714	1108	0.66	29.40 ± 0.39	0.0486 ± 0.0011	215.7 ± 2.8			
SK_118	0.97	171	98	0.59	34.32 ± 0.87	0.0382 ± 0.0068	185.1 ± 4.6			
SK_119	0.00	445	129	0.30	29.14 ± 0.52	0.0525 ± 0.0023	217.5 ± 3.8			
SK_120	0.00	64	40	0.65	2.72 ± 0.04	0.1325 ± 0.0033	2015.5 ± 28.1	2133 ± 42	5.51	
SK_121	0.00	60	42	0.71	61.01 ± 2.74	0.0532 ± 0.0079	104.8 ± 4.7			
SK_122	1.01	243	157	0.66	24.08 ± 0.43	0.0471 ± 0.0053	262.3 ± 4.6			
SK_123	0.41	423	367	0.89	33.64 ± 0.63	0.0509 ± 0.0050	188.8 ± 3.5			
SK_124	0.34	647	266	0.42	32.28 ± 0.51	0.0475 ± 0.0028	196.7 ± 3.1			
SK_125	0.00	983	1550	1.62	2.79 ± 0.04	0.1262 ± 0.0012	1972.4 ± 21.4	2047 ± 16	3.64	
SK_126	0.27	1014	263	0.27	35.66 ± 0.51	0.0485 ± 0.0019	178.3 ± 2.5			
SK_127	0.00	1762	615	0.36	18.41 ± 0.25	0.0538 ± 0.0009	341.0 ± 4.5			
SK_128	1.18	235	212	0.92	24.22 ± 0.45	0.0470 ± 0.0062	260.8 ± 4.8			
SK_129	0.15	897	347	0.40	30.85 ± 0.52	0.0489 ± 0.0023	205.6 ± 3.4			
SK_130	0.00	244	92	0.39	3.17 ± 0.05	0.1116 ± 0.0016	1766.6 ± 23.7	1826 ± 26	3.25	
SK_131	0.12	390	25	0.06	36.87 ± 0.62	0.0514 ± 0.0027	172.5 ± 2.9			
SK_132	0.00	201	91	0.46	31.09 ± 0.66	0.0575 ± 0.0033	204.1 ± 4.3			discordant
SK_133	0.00	52	27	0.53	23.72 ± 0.86	0.0495 ± 0.0056	266.2 ± 9.4			
SK_134	0.01	302	59	0.20	3.21 ± 0.05	0.1160 ± 0.0020	1748.8 ± 23.0	1897 ± 30	7.81	
SK_135	0.00	493	326	0.68	29.47 ± 0.53	0.0523 ± 0.0019	215.1 ± 3.8			
SK_136	0.00	139	86	0.64	35.23 ± 0.92	0.0466 ± 0.0037	180.4 ± 4.6			
SK_137	0.00	383	134	0.36	25.77 ± 0.43	0.0484 ± 0.0019	245.4 ± 4.0			
SK_138	0.00	500	111	0.23	7.58 ± 0.11	0.1018 ± 0.0017	798.9 ± 10.8	1659 ± 30	51.84	discordant
SK_139	0.00	110	79	0.74	35.53 ± 0.92	0.0486 ± 0.0047	179.0 ± 4.6			
SK_140	0.07	573	99	0.18	3.61 ± 0.04	0.1305 ± 0.0019	1575.2 ± 16.7	2106 ± 26	25.20	discordant
SK_141	0.00	188	112	0.61	33.35 ± 0.88	0.0463 ± 0.0034	190.4 ± 4.9			
SK_142	0.10	217	57	0.27	32.35 ± 0.71	0.0494 ± 0.0047	196.2 ± 4.2			
SK_143	0.12	510	288	0.58	30.08 ± 0.54	0.0509 ± 0.0044	210.8 ± 3.7			
NN_001	0.43	282	106	0.39	35.05 ± 0.82	0.0532 ± 0.0043	181.3 ± 4.2			
NN_002	0.08	417	64	0.16	2.78 ± 0.06	0.1373 ± 0.0022	1978.4 ± 34.9	2195 ± 27	9.87	
NN_003	2.70	316	434	1.41	34.93 ± 0.98	0.0389 ± 0.0111	182.0 ± 5.0			
NN_004	0.26	105	111	1.09	32.31 ± 1.06	0.0469 ± 0.0124	196.5 ± 6.4			
NN_005	0.14	142	96	0.69	2.85 ± 0.06	0.1333 ± 0.0034	1938.0 ± 32.9	2143 ± 44	9.57	
NN_006	0.29	127	59	0.47	26.41 ± 0.71	0.0531 ± 0.0058	239.6 ± 6.3			
NN_007	1.24	166	129	0.80	25.44 ± 0.58	0.0401 ± 0.0065	248.5 ± 5.6			
NN_008	0.00	348	123	0.36	3.21 ± 0.06	0.1164 ± 0.0020	1746.7 ± 29.0	1903 ± 31	8.21	
NN_009	0.00	819	440	0.55	15.75 ± 0.26	0.0556 ± 0.0014	396.9 ± 6.4			
NN_010	0.45	157	157	1.03	3.49 ± 0.06	0.1091 ± 0.0049	1623.3 ± 24.3	1785 ± 80	9.06	
NN_011	0.93	1125	453	0.41	4.21 ± 0.06	0.1113 ± 0.0016	1373.1 ± 17.4	1822 ± 25	24.64	discordant
NN_012	0.38	389	54	0.14	3.26 ± 0.05	0.1165 ± 0.0018	1722.5 ± 20.9	1904 ± 28	9.53	
NN_013	0.00	238	87	0.37	35.12 ± 0.80	0.0479 ± 0.0033	181.0 ± 4.1			
NN_014	0.57	217	172	0.82	29.31 ± 0.77	0.0466 ± 0.0077	216.3 ± 5.6			
NN_015	0.71	244	114	0.48	34.48 ± 0.86	0.0459 ± 0.0056	184.3 ± 4.5			
NN_016	0.00	475	209	0.45	16.57 ± 0.27	0.0552 ± 0.0017	377.7 ± 5.9			
NN_017	0.06	326	31	0.10	3.16 ± 0.04	0.1143 ± 0.0016	1772.1 ± 20.7	1870 ± 26	5.23	
NN_018	0.09	592	49	0.09	3.35 ± 0.04	0.1133 ± 0.0014	1683.2 ± 19.4	1854 ± 21	9.21	
NN_019	0.44	142	44	0.32	32.57 ± 0.80	0.0471 ± 0.0060	194.9 ± 4.7			
NN_020	0.00	41	34	0.86	24.61 ± 0.93	0.0460 ± 0.0074	256.8 ± 9.5			
NN_021	0.24	376	148	0.40	38.84 ± 0.91	0.0473 ± 0.0045	163.9 ± 3.8			

Table A1. Continued.

Labels	$^{206}Pb_c$ [(1)] (%)	U (ppm)	Th (ppm)	Th/U	$^{238}U/^{206}Pb^*$ [(1)]	$^{207}Pb^*/^{206}Pb^*$ [(1)]	$^{238}U/^{206}Pb^*$ age[(1)] (Ma)	$^{207}Pb^*/^{206}Pb^*$ age[(1)] (Ma)	Disc [(2)] (%)	Remarks
NN_022	0.07	377	15	0.04	28.48 ± 0.55	0.0502 ± 0.0026	222.4 ± 4.2			
NN_023	3.70	33	23	0.70	21.56 ± 0.93	0.0349 ± 0.0183	292.3 ± 12.4			
NN_024	0.28	633	346	0.56	38.10 ± 0.59	0.0447 ± 0.0034	167.0 ± 2.5			
NN_025	0.12	138	67	0.50	30.08 ± 0.74	0.0521 ± 0.0067	210.8 ± 5.1			
NN_026	0.00	387	152	0.40	37.28 ± 0.72	0.0484 ± 0.0024	170.6 ± 3.2			
NN_027	0.20	56	18	0.32	22.10 ± 0.71	0.0574 ± 0.0091	285.3 ± 9.0			
NN_028	0.00	125	90	0.74	23.85 ± 0.63	0.0445 ± 0.0041	264.8 ± 6.8			
NN_029	0.00	113	48	0.44	30.79 ± 0.85	0.0552 ± 0.0052	206.0 ± 5.6			
NN_030	0.00	503	59	0.12	3.25 ± 0.05	0.1127 ± 0.0014	1728.2 ± 23.4	1844 ± 22	6.28	
NN_031	0.13	153	86	0.58	2.27 ± 0.04	0.1623 ± 0.0037	2357.0 ± 38.2	2481 ± 38	5.00	
NN_032	0.00	77	42	0.56	25.96 ± 0.86	0.0638 ± 0.0069	243.7 ± 8.0			
NN_033	0.00	1129	88	0.08	3.83 ± 0.06	0.1107 ± 0.0013	1494.8 ± 21.0	1813 ± 21	17.55	discordant
NN_034	1.27	135	108	0.82	27.35 ± 1.00	0.0464 ± 0.0098	231.5 ± 8.3			
NN_035	0.44	187	116	0.64	65.63 ± 2.19	0.0561 ± 0.0120	97.5 ± 3.2			
NN_036	0.80	429	201	0.48	3.15 ± 0.05	0.1068 ± 0.0033	1778.0 ± 22.4	1747 ± 55	− 1.77	
NN_037	0.08	133	114	0.88	2.64 ± 0.05	0.1593 ± 0.0040	2073.4 ± 32.4	2449 ± 42	15.34	discordant
NN_038	0.00	826	551	0.68	36.45 ± 0.86	0.0501 ± 0.0022	174.5 ± 4.0			
NN_039	2.75	92	74	0.82	33.36 ± 1.32	0.0412 ± 0.0172	190.4 ± 7.4			
NN_040	0.00	622	200	0.33	27.16 ± 0.57	0.0513 ± 0.0022	233.1 ± 4.8			
NN_041	0.00	491	361	0.75	35.33 ± 0.74	0.0569 ± 0.0028	179.9 ± 3.7			discordant
NN_042	0.34	352	342	1.00	25.51 ± 0.56	0.0475 ± 0.0071	247.9 ± 5.3			
NN_043	0.45	46	26	0.57	25.07 ± 1.25	0.0694 ± 0.0167	252.2 ± 12.4			
NN_044	1.54	126	75	0.61	27.40 ± 0.83	0.0426 ± 0.0092	231.0 ± 6.9			
NN_045	0.35	516	310	0.62	17.03 ± 0.32	0.0528 ± 0.0038	367.8 ± 6.7			
NN_046	1.06	89	74	0.85	27.85 ± 1.15	0.0603 ± 0.0139	227.4 ± 9.3			
NN_047	0.00	401	183	0.47	27.46 ± 0.72	0.0554 ± 0.0029	230.6 ± 5.9			
NN_048	2.27	324	143	0.45	34.82 ± 0.79	0.0660 ± 0.0064	182.5 ± 4.1			discordant
NN_049	0.05	724	464	0.66	26.59 ± 0.51	0.0498 ± 0.0035	238.0 ± 4.5			
NN_050	0.58	244	172	0.72	35.47 ± 0.86	0.0483 ± 0.0073	179.2 ± 4.3			
NN_051	0.36	158	68	0.44	2.02 ± 0.04	0.2155 ± 0.0043	2597.7 ± 42.3	2949 ± 31	11.91	
NN_052	0.50	665	257	0.40	36.77 ± 0.80	0.0486 ± 0.0041	173.0 ± 3.7			
NN_053	0.00	799	189	0.24	29.47 ± 0.62	0.0524 ± 0.0022	215.1 ± 4.5			
NN_054	0.00	304	160	0.54	34.33 ± 0.84	0.0540 ± 0.0035	185.1 ± 4.4			
NN_055	0.00	509	473	0.95	23.88 ± 0.47	0.0490 ± 0.0028	264.5 ± 5.1			
NN_056	1.34	141	89	0.65	32.90 ± 1.11	0.0492 ± 0.0128	193.0 ± 6.4			
NN_057	0.00	192	154	0.82	31.32 ± 0.91	0.0476 ± 0.0048	202.6 ± 5.8			
NN_058	0.05	312	117	0.39	25.61 ± 0.50	0.0533 ± 0.0046	246.9 ± 4.7			
NN_059	0.08	136	56	0.42	24.07 ± 0.64	0.0510 ± 0.0070	262.4 ± 6.8			
NN_060	0.00	140	84	0.61	24.88 ± 0.60	0.0527 ± 0.0049	254.0 ± 6.0			
NN_061	0.00	235	141	0.62	24.90 ± 0.54	0.0506 ± 0.0033	253.9 ± 5.4			
NN_062	0.00	368	150	0.42	36.85 ± 0.81	0.0438 ± 0.0029	172.6 ± 3.8			
NN_063	0.71	424	174	0.42	31.87 ± 0.64	0.0494 ± 0.0046	199.2 ± 4.0			
NN_064	0.00	290	176	0.62	3.19 ± 0.05	0.1150 ± 0.0020	1759.0 ± 23.6	1881 ± 31	6.49	
NN_065	0.00	307	96	0.32	37.07 ± 1.01	0.0507 ± 0.0038	171.6 ± 4.6			
NN_066	0.00	93	68	0.75	23.39 ± 0.84	0.0539 ± 0.0056	269.8 ± 9.5			
NN_067	2.10	1333	676	0.52	24.94 ± 0.40	0.0455 ± 0.0029	253.4 ± 4.0			
NN_068	0.00	91	51	0.57	60.02 ± 2.66	0.0476 ± 0.0071	106.5 ± 4.7			
NN_069	0.22	120	89	0.76	26.11 ± 0.79	0.0443 ± 0.0093	242.3 ± 7.2			
NN_070	0.00	186	180	0.99	29.70 ± 0.74	0.0490 ± 0.0036	213.5 ± 5.3			
NN_071	0.33	371	145	0.40	32.35 ± 0.70	0.0479 ± 0.0042	196.2 ± 4.2			
NN_072	0.76	255	75	0.30	3.06 ± 0.05	0.1356 ± 0.0027	1822.6 ± 28.3	2173 ± 34	16.12	discordant
NN_073	0.38	698	508	0.75	31.67 ± 0.62	0.0443 ± 0.0047	200.4 ± 3.8			
NN_074	0.00	909	120	0.14	3.06 ± 0.04	0.1140 ± 0.0014	1825.3 ± 20.7	1866 ± 21	2.18	
NN_075	0.00	114	77	0.70	25.25 ± 0.81	0.0471 ± 0.0041	250.4 ± 7.8			
NN_076	0.27	84	53	0.65	28.33 ± 1.02	0.0457 ± 0.0120	223.6 ± 7.9			
NN_077	0.13	691	314	0.47	31.63 ± 0.54	0.0476 ± 0.0035	200.6 ± 3.3			
NN_078	0.01	337	63	0.19	3.19 ± 0.06	0.1129 ± 0.0021	1756.0 ± 26.7	1848 ± 33	4.98	
NN_079	0.00	178	94	0.54	24.42 ± 0.61	0.0486 ± 0.0040	258.7 ± 6.3			
NN_080	0.00	339	337	1.02	31.67 ± 0.63	0.0460 ± 0.0022	200.4 ± 3.9			
NN_081	1.37	378	161	0.44	33.18 ± 0.62	0.0428 ± 0.0053	191.4 ± 3.5			
NN_082	0.49	141	118	0.86	32.98 ± 0.91	0.0515 ± 0.0097	192.6 ± 5.2			
NN_083	0.04	62	32	0.52	30.78 ± 1.42	0.0627 ± 0.0132	206.1 ± 9.3			
NN_084	2.23	511	118	0.24	38.49 ± 0.89	0.0472 ± 0.0059	165.3 ± 3.8			
NN_085	0.00	334	196	0.60	3.07 ± 0.05	0.1128 ± 0.0018	1818.1 ± 23.6	1845 ± 29	1.46	
NN_086	0.03	456	216	0.49	16.18 ± 0.25	0.0524 ± 0.0031	386.5 ± 5.7			

Table A1. Continued.

Labels	$^{206}Pb_c$ (1) (%)	U (ppm)	Th (ppm)	Th/U	$^{238}U/^{206}Pb^{*(1)}$	$^{207}Pb^{*}/^{206}Pb^{*(1)}$	$^{238}U/^{206}Pb^{*}$ age(1) (Ma)	$^{207}Pb^{*}/^{206}Pb^{*}$ age(1) (Ma)	Disc (2) (%)	Remarks
NN_087	0.08	592	174	0.30	31.49 ± 0.54	0.0483 ± 0.0031	201.6 ± 3.4			
NN_088	0.00	242	84	0.36	3.08 ± 0.05	0.1140 ± 0.0019	1813.9 ± 23.3	1865 ± 30	2.74	
NN_089	0.00	157	78	0.51	32.18 ± 0.78	0.0534 ± 0.0047	197.3 ± 4.7			
NN_090	0.00	245	91	0.38	28.56 ± 0.52	0.0460 ± 0.0029	221.8 ± 3.9			
NN_091	2.63	706	399	0.58	34.06 ± 0.56	0.0459 ± 0.0042	186.5 ± 3.0			
NN_092	0.00	248	61	0.25	3.82 ± 0.05	0.1119 ± 0.0019	1497.9 ± 17.0	1831 ± 31	18.19	discordant
NN_093	0.19	96	68	0.72	23.87 ± 0.63	0.0489 ± 0.0090	264.6 ± 6.8			
NN_094	0.00	198	89	0.46	3.02 ± 0.04	0.1143 ± 0.0016	1844.5 ± 23.5	1869 ± 26	1.31	
NN_095	0.40	138	62	0.46	30.08 ± 0.75	0.0411 ± 0.0066	210.8 ± 5.2			
NN_096	0.00	557	307	0.57	33.81 ± 0.56	0.0484 ± 0.0020	187.9 ± 3.1			
NN_097	0.00	186	80	0.44	37.29 ± 1.03	0.0540 ± 0.0041	170.6 ± 4.6			
NN_098	0.00	230	144	0.64	34.23 ± 0.76	0.0553 ± 0.0030	185.6 ± 4.0			
NN_099	0.14	294	128	0.45	33.15 ± 0.75	0.0482 ± 0.0055	191.6 ± 4.3			
NN_100	0.00	201	230	1.17	52.00 ± 1.61	0.0574 ± 0.0054	122.8 ± 3.8			
NN_101	0.19	128	77	0.62	24.44 ± 0.57	0.0500 ± 0.0077	258.5 ± 5.9			
NN_102	0.00	268	90	0.34	30.17 ± 0.60	0.0519 ± 0.0030	210.2 ± 4.1			
NN_103	0.11	543	229	0.43	14.99 ± 0.24	0.0536 ± 0.0029	416.4 ± 6.5			
NN_104	0.00	210	47	0.23	2.93 ± 0.05	0.1138 ± 0.0020	1895.3 ± 26.3	1862 ± 31	− 1.79	
NN_105	0.00	453	217	0.49	3.11 ± 0.04	0.1158 ± 0.0016	1798.1 ± 22.3	1893 ± 25	5.01	
NN_106	0.00	138	61	0.45	23.76 ± 0.47	0.0535 ± 0.0030	265.8 ± 5.1			
NN_107	0.41	429	164	0.39	35.89 ± 0.65	0.0468 ± 0.0039	177.2 ± 3.2			
NN_108	0.04	382	250	0.67	3.66 ± 0.06	0.1092 ± 0.0025	1555.5 ± 21.5	1788 ± 41	13.00	
NN_109	0.00	19	7	0.40	23.27 ± 1.28	0.0484 ± 0.0111	271.3 ± 14.6			
NN_110	0.64	134	55	0.42	30.63 ± 0.96	0.0434 ± 0.0071	207.1 ± 6.4			
NN_111	0.00	226	107	0.48	3.01 ± 0.05	0.1138 ± 0.0018	1847.5 ± 26.7	1863 ± 29	0.83	
NN_112	0.15	399	46	0.12	3.14 ± 0.04	0.1102 ± 0.0016	1779.8 ± 22.1	1804 ± 26	1.34	
NN_113	0.50	169	47	0.28	57.86 ± 2.12	0.0532 ± 0.0083	110.5 ± 4.0			
NN_114	0.25	293	120	0.42	24.69 ± 0.51	0.0486 ± 0.0043	255.9 ± 5.2			
NN_115	0.80	534	273	0.52	35.01 ± 0.67	0.0510 ± 0.0048	181.5 ± 3.4			
NN_116	0.11	872	74	0.09	3.23 ± 0.05	0.1206 ± 0.0016	1737.8 ± 23.0	1965 ± 24	11.56	
NN_117	0.71	124	58	0.48	31.92 ± 0.94	0.0441 ± 0.0078	198.9 ± 5.8			
NN_118	0.05	271	170	0.65	36.74 ± 0.86	0.0453 ± 0.0062	173.1 ± 4.0			
NN_119	0.00	231	172	0.76	34.51 ± 0.85	0.0464 ± 0.0040	184.1 ± 4.4			
NN_120	0.09	142	85	0.61	3.09 ± 0.06	0.1143 ± 0.0030	1809.3 ± 29.6	1871 ± 47	3.30	
NN_121	0.00	164	79	0.50	2.62 ± 0.05	0.1339 ± 0.0022	2083.7 ± 32.0	2151 ± 28	3.13	
NN_122	0.00	353	135	0.39	32.16 ± 0.67	0.0572 ± 0.0028	197.4 ± 4.0			discordant
NN_123	0.00	42	20	0.48	25.02 ± 1.00	0.0566 ± 0.0077	252.6 ± 9.9			
NN_124	1.26	971	343	0.36	16.38 ± 0.24	0.0544 ± 0.0019	382.0 ± 5.5			
NN_125	0.00	195	123	0.64	30.90 ± 0.72	0.0521 ± 0.0035	205.3 ± 4.7			
NN_126	0.00	648	1189	1.88	29.50 ± 0.52	0.0496 ± 0.0019	214.9 ± 3.8			
NN_127	0.13	2289	319	0.14	16.74 ± 0.26	0.0537 ± 0.0010	374.0 ± 5.7			
NN_128	0.88	445	270	0.62	33.15 ± 0.64	0.0453 ± 0.0048	191.6 ± 3.6			
NN_129	0.00	428	214	0.51	3.15 ± 0.05	0.1142 ± 0.0015	1776.9 ± 22.7	1868 ± 24	4.87	
NN_130	0.00	262	109	0.43	30.38 ± 0.68	0.0485 ± 0.0027	208.8 ± 4.6			
NN_131	0.17	118	62	0.54	23.55 ± 0.63	0.0444 ± 0.0062	268.1 ± 7.0			
NN_132	0.00	215	89	0.42	25.64 ± 0.56	0.0461 ± 0.0025	246.6 ± 5.3			
NN_133	0.09	813	308	0.39	39.01 ± 0.80	0.0520 ± 0.0029	163.2 ± 3.3			
NN_134	0.16	120	81	0.69	31.65 ± 0.91	0.0510 ± 0.0083	200.5 ± 5.7			
NN_135	0.00	75	39	0.53	34.24 ± 1.12	0.0499 ± 0.0058	185.6 ± 6.0			
NN_136	1.36	221	151	0.70	25.36 ± 0.53	0.0431 ± 0.0062	249.3 ± 5.1			
NN_137	0.00	615	358	0.60	26.23 ± 0.47	0.0502 ± 0.0018	241.2 ± 4.2			
NN_138	0.38	153	86	0.58	34.09 ± 0.94	0.0552 ± 0.0083	186.4 ± 5.1			
NN_139	0.07	157	105	0.69	3.73 ± 0.06	0.1122 ± 0.0033	1532.1 ± 21.4	1837 ± 53	16.60	discordant
NN_140	0.66	438	287	0.67	35.29 ± 0.68	0.0445 ± 0.0046	180.2 ± 3.4			
NN_141	2.50	1426	624	0.45	32.56 ± 0.51	0.0513 ± 0.0031	195.0 ± 3.0			
NN_142	0.00	68	31	0.47	25.65 ± 0.75	0.0671 ± 0.0072	246.6 ± 7.1			discordant
NN_143	0.29	168	165	1.01	24.35 ± 0.58	0.0508 ± 0.0077	259.4 ± 6.0			
NN_144	0.00	139	112	0.82	23.72 ± 0.65	0.0464 ± 0.0032	266.2 ± 7.2			
NN_145	0.20	701	373	0.55	2.74 ± 0.03	0.1215 ± 0.0019	2003.5 ± 21.2	1980 ± 27	− 1.19	
NN_146	0.00	253	84	0.34	2.96 ± 0.05	0.1107 ± 0.0018	1875.5 ± 25.2	1811 ± 30	− 3.56	
NN_147	0.00	286	126	0.45	16.12 ± 0.30	0.0563 ± 0.0022	388.0 ± 7.0			
NN_148	0.00	209	211	1.03	3.56 ± 0.06	0.1121 ± 0.0021	1595.8 ± 23.9	1835 ± 34	13.04	

Errors are 1-sigma; Pb_c and Pb^* indicate the common and radiogenic portions, respectively.

(1) Common Pb corrected by assuming $^{206}Pb/^{238}U$–$^{208}Pb/^{232}Th$ age-concordance

(2) The degree of discordance for an analyzed spot indicates the chronological difference between the two ages determined by Pb–Pb and U–Pb methods, and is defined as $\{1 - (^{238}U/^{206}Pb^*\ \text{age})/(^{207}Pb^*/^{206}Pb^*\ \text{age})\} \times 100$ (%) (e.g., Song *et al.*, 1996).